SCIENTIFIC COMMITTEE

SEVENTEENTH REGULAR SESSION

Online meeting

11–19 August 2021

Background analyses for the 2021 stock assessment of Southwest Pacific swordfish

WCPFC-SC17-2021/SA-IP-07

30 July 2021

N. Ducharme-Barth[1], T. Peatman[2], and P. Hamer[1]

[1]Oceanic Fisheries Programme, Pacific Community (SPC), Nouméa, New Caledonia
[2]Independent fisheries consultant for the Pacific Community (SPC), Ocean Fisheries Programme (OFP)

Contents

Executive Summary

This paper provides details of analyses undertaken to construct input data and biological parameters for the 2021 southwest Pacific Ocean swordfish stock assessment. Several discrete topics are presented in-turn, and further detail is provided than could be included in the main assessment report (Ducharme-Barth et al., 2021).

Fisheries definitions for the 2021 assessment were very similar to the 2017 assessment, and minor modifications included: changing which fisheries Vanuatu vessels were assigned to; the merging of two temporally split distant water fishing nation fisheries; and the establishment of a European Union fishery in region 1. The more significant change was the adoption of the "index fisheries approach", to be consistent with recent Western and Central Pacific Ocean tuna assessments, resulting in 13 extraction fisheries and 13 index fisheries.

A number of Bayesian statistical models were constructed to improve the modelling of biological functions necessary for the assessment; growth curves, maturity functions, the length-weight relationship and the sex-ratio at length. The resulting posterior distributions were sampled, and using established life-history relationships, formed the range of input values for the structural uncertainty grid of the assessment (the ensemble approach; Ducharme-Barth and Vincent, 2021).

Longline operational data from three Distant Water Fishing Nation (DWFN) fleets were standardized using the VAST spatiotemporal modelling framework. Indices for the European Union (i.e. Spanish), Japanese, and Chinese Taipei longline fleets operating in the south Pacific were created. Temporal and spatial partitioning of the data resulted in 11 different indices.

Finally, the method of spatial reweighting the size composition data that has been used in other recent assessments in the region was adopted. Size compositions were reweighted by catch for the extraction fisheries to ensure that catches were removed from the modelled population at appropriate sizes, while compositions for index fisheries were reweighted by CPUE to better reflect the changes in size structure of the underlying population.

1 Introduction

There are often substantial changes made between successive assessments of stocks in the Western and Central Pacific Ocean (WCPO). These can be attributed to the provision of additional fisheries or biological data, implementation of recently developed features of Multifan-CL (MFCL) or general developments in the stock assessment field subsequent to the previous assessment, amongst others. This paper serves as a reference to the changes made between the 2017 and 2021 assessments of southwest Pacific swordfish, with a focus on the inputs to the stock assessment, rather than the modifications to the structural components of the model itself that are covered in the main assessment report (Ducharme-Barth et al., 2021).

There are a large number of inputs required for a fully age-structured stock assessment, ranging from data components to biological parameters. Consequently, this report comprises several discrete topics, where the objective is to provide a level of background detail not possible in the main assessment report for topics that do not warrant stand-alone papers. These topics can be briefly summarised in-turn as:

- Changes to fisheries structure (section 2); An outline of all the changes to fisheries definitions made subsequent to the 2017 assessment.
- Estimation of biological functions (section 3); A summary of the suite of analyses undertaken to estimate the length-weight, maturity, sex-ratio at length and growth functions used in the assessment, which together form the basis of the ensemble model approach presented by Ducharme-Barth and Vincent (2021) that was utilised for the 2021 assessment.
- Standardisation of CPUE indices (section 4); Describes the process of estimating the set of standardised CPUE indices that are used to inform the model of changes in relative abundance of the stock over the assessment period.
- Preparation of size frequency data (section 5); Describes the process of spatially reweighting the length composition data to ensure that it is representative of the sizes of fish in the population, or alternatively, those being extracted from the stock.

The reader should also refer to the main assessment report (Ducharme-Barth et al., 2021) for stock assessment conclusions and recommendations based on the analyses presented herein.

2 Fisheries definitions

The regional and fisheries structures for the assessment are addressed in detail in Ducharme-Barth et al. (2021), and this document therefore focuses on the changes made to fisheries definitions since the 2017 assessment (Takeuchi et al., 2017). It also serves as a repository for the fisheries summary plots (see Appendix; Fig.s A1-1–A1-25). The 2021 assessment adopted the “index fisheries approach” that involves defining separate “extraction” and “index” fisheries, a feature which has been applied in all recent WCPO tuna assessments (e.g. Ducharme-Barth et al., 2020; Vincent et al., 2020; Castillo-Jordan et al., 2021). The fisheries definitions of the diagnostic case model are provided in the main assessment report (Table 2; Ducharme-Barth et al., 2021).

This partitioning of extraction and index fisheries was the most significant change from the previous assessment and the structure of the extraction fisheries (fisheries 1–13; Figs. A1-1–A1-25) is fairly consistent with the full set of fisheries in 2017. The exceptions to this were:

- All Vanuatu fishing activity was shifted from the Pacific Island Countries and Territories (PICT) fisheries (F6 - region R1, F12 - R2N, F13 - R2C) to the Distant Water Fishing Nation (DWFN) fisheries (F1–3 and F7–8) as those vessels operate in a manner more similar to the latter.
- The EU vessels operating in region 1 were removed from the PICT fishery (F6) and formed their own, new fishery (F5). This was related to their operational characteristics (high prevalence of swordfish targeting) as well as differences in data provision compared to other fleets. Catches for this fishery were included in the assessment as catch-in-weight rather than numbers, to reflect this provision (this feature was also applied to the previously established EU fishery, F11, in R2).
- In 2017, the DWFN fishery in R2C was split into two (F7 and F8; Table 1 of Takeuchi et al., 2017) in an attempt to alleviate concerns about temporal changes in catchability of this fleet. The adoption of the index fishery approach for the current assessment precludes the need to split this fishery and consequently the former F7 and F8 are merged to form a single fishery - F8 (Table 2; Ducharme-Barth et al., 2021).
- The previous assessment noted conflict between the Australian length and weight composition data. The length-composition data for the Australian fisheries (F4 and F14) were excluded based on discussions at the PAW which suggested that the weight frequency data (obtained from port-sampling) would be more representative (Hamer et al., 2021).

Given that the establishment of the EU fishery in R2C offsets the reduction in fishery number by one from the last assessment (due to the amalgamation of the DWFN fishery in the same sub-region that was previously spit into separate fisheris for the early and late time-periods), 13 extraction fisheries are again used in the assessment.

The basis for the index fishery approach is detailed in Ducharme-Barth et al. (2021) and the consequences for CPUE indices are outlined in Section 4. Briefly, the approach aims to separate extraction fisheries, where the fish caught are taken from the modelled stock at the correct amounts and at appropriate sizes, from the index fisheries, where size and CPUE data that is more representative of trends in the population are modelled. These fisheries receive the standardised CPUE indices (Section 4) and size data that has been spatially reweighted to be representative of biomass of the stock rather than the catch (Section 5). This resulted in 13 such fisheries specific to certain time periods and sub-regions, and incorporating data from vessels of particular flags. Summaries for these fisheries are shown in the appendix (Figs. A1-14–A1-25).

3 Estimation of biological functions

All modelling of the estimated biological parameters was done using the STAN probabilistic programming language as implemented in R using rstan (STAN Development Team, 2021). For each model, 50,000 samples were drawn from 8 separate chains, each with random initial conditions. Chains were assessed for convergence, and all models were found to be well determined on the basis of standard Hamiltonian Monte Carlo diagnostics (e.g. divergences, maximum tree depth, and energy).

3.1 Length-weight relationships

The relationship between length and weight of fish was modelled using sex-specific power functions. The standard implementation of these models was utillised and consisted of a simple regression of weight (w_i) against length (l_i) of each fish i, on the log scale, e.g.

$$\acute{w}_i \sim Normal(\log\alpha_{j[i]} + \beta_{j[i]} \times \log(l_i), \sigma)$$
$$w_i = exp(\acute{w}_i)$$

where $\alpha_{j[i]}$ and $\beta_{j[i]}$ are intercept and slope terms specific to the sex j of fish i. Both sexes assumed identical, but sex-specific, priors for all parameters. Priors were specified to be relatively uninformative with a large CV on the log-scale (0.5). The prior for the regression standard deviation, σ, was $\log(\sigma) \sim \text{Normal}(\log(0.5), 0.5)$, for the regression intercept parameter α_j $\log(\alpha_j) \sim \text{Normal}(\log(1e-05), 0.5)$ and for the regression slope parameter $\log(\beta_j) \sim \text{Normal}(\log(3), 0.5)$. The prior means were taken to be similar to the previously assumed values for the corresponding parameters.

In order to maximize the observations available for analysis, all paired lengths (Lower Jaw Fork Length; LJFL cm) and whole weights (kg) for individual fish that were obtained from observer records in SPC holdings south of 5°N, and up through the year 2019 were included. While this meant that $\sim 22\%$ of observations were technically outside of the model region, the distribution of paired lengths and weights from these fish did not appear to differ from those that were measured within the model region. A sensitivity to excluding these fish did not result in meaningful differences to the estimated parameters. For fish that were not measured according to the standard LJFL or WW, these were converted to the appropriate measurement type according to SPC conversion factors. A total of 5,721 individual fish were available and consisted of 2,451 males and 3,270 females.

3.2 Maturity functions

Sex-specific maturity-at-length relationships were investigated using biological data collected from longline caught swordfish in the Coral Sea by Young et al. (2003). A total of 916 individual fish were sampled over the period 1999–2001, consisting of 231 males and 685 females. The lengths of each fish were recorded and histological samples were analysed to assess the sexual maturity of each fish, as outlined in Farley et al. (2016). Only female fish were considered for further analysis.

The resulting dataset consisted of binary data where maturity of fish i, m_i, was determined to be either mature (1) or immature (0), and data were modelled using a modified logistic regression against length l_i. It is occasionally difficult to accurately determine maturity status of some fish, depending on the timing in the spawning season. The modifications to the logistic model accommodated errors in determination of maturity (McInturff et al., 2004), either in the form of false positives (designated mature, when immature) and false negatives (designated immature, when mature). The set of equations for this approach are given by:

$$m_i \sim \text{Bernoulli}(p_i)$$
$$p_i = \eta_i \pi_i + (1 - \theta_i)(1 - \pi_i)$$
$$\pi_i = \frac{1}{(1 + \exp(\phi_i \times (L_i - \tau_i)))}$$

where the probability of being mature p_i involves adjustment of the usual function represented by π_i (linear relationship on the logit scale) using the parameters η and θ. These parameters are equivalent to the sensitivity and specificity of the classification problem, respectively. These are given uninformative priors $\text{logit}(\theta) \sim \text{Normal}(0, 1)$, and $\text{logit}(\eta) \sim \text{Normal}(0, 1)$.

3.3 Sex ratio at length

The sex ratio at length data were modelled using a variant of the generalised logistic function. The data comprised all individual fish from observer records in SPC holdings south of 5°N, and up through the year 2019, and consisted of 47,506 individual fish of which ∼ 11% were technically outside of the assessment region. A sensitivity to excluding these fish did not result in meaningful differences to the estimated parameters, nor in the resulting sex-ratio at length relationship. Data was modelled as a binary variable s_i, where 0's and 1's were males (n = 22,089) and females (n = 25,417), respectively. The probability of fish i being female, p_i, was modelled as a function of fish length l_i using the following five-parameter model:

$$s_i \sim \text{Bernoulli}(p_i)$$
$$p_i = \omega + \frac{\lambda - \omega}{(1 + \exp(-\kappa \times (l_i - \delta)))^{\nu}}$$

where ω is a lower asymptote with prior $\text{logit}(\omega) \sim \text{Normal}(0, 0.05)$, λ is an upper asymptote with $\text{logit}(\lambda) \sim \text{Normal}(1, 1)$, κ is the slope of the function with length, with a prior of $\kappa \sim \text{Normal}(0, 0.1)$, δ is a parameter that determines the fish length (cm) at which the inflection point of the function occurs, which had a prior of $\delta \sim \text{Normal}(150, 150)$, and ν which allows asymmetry in the form of the function on either side of the inflection point, and was given a prior of $\nu \sim \text{Normal}(0, 1)$. All priors were relatively uniformative except for the prior on ω which was very informative (0.5 on logit scale) based on the assumption that sex-ratio at small size (e.g. birth) was 50:50.

3.4 Sex-specific growth function

This year, CSIRO investigated estimating a decimal age for swordfish using age estimates (counts of opaque zones) and otolith measurement data from Farley et al. (2016). A decimal age was calculated for each fish using the methods developed for western and central Pacific bigeye and yellowfin (Farley et al., 2020). First, the relationship between (sectioned) otolith size and daily age was used to estimate the age of the fish when the first annual opaque zone was deposited in the otolith. Second, the number of complete annual increments in the otolith was estimated. Finally, the time elapsed (proportion of a year) after the last counted opaque zone was deposited and when the fish was caught was estimated, based on the marginal increment as a proportion of the mean size of the complete annulus for that age group. Total age was estimated by adding together the age components estimated in each step.

The growth curve was modelled using a standard sex-specific von Bertalanffy function, assuming uniformative priors centered on the values from (Farley et al., 2016), that was fitted to the age and length dataset from the decimal aged fish:

$$l_i \sim \text{Normal}(L_{\infty,j[i]} \left(1 - \exp\left(-k_{j[i]} \left(a_i - t0_j\right)\right)\right), \sigma_l)$$

where; l_i is the length (LJFL) of fish i for a fish at age a (annual), σ_l is the standard deviation of length which has a prior of $log(\sigma_l) \sim \text{Normal}(\log(26), 0.5)$, $L_{\infty,j}$ is the sex-specific average length of fish at hypothetical infinite ages for sex j, which had priors $\log(L_{\infty,j}) \sim \text{Normal}(\mu_j^{L\infty}, \sigma_j^{L\infty})$ where $\mu^{L\infty}$ was log(212) and log(276) for males and females respectively, and $\sigma^{L\infty}$ was 0.5 for both sexes, and k_j is the sex-specific von Bertalanffy growth coefficient which had priors $\log(k_{\infty,j}) \sim \text{Normal}(\mu_j^k, \sigma_j^k)$ where μ^k was log(0.24) and log(0.16) for males and females respectively, and σ^k was 0.5 for both sexes and $t0_j$ is the hypothetical age of a fish when length is 0, which was again sex-specific and had priors of $t0_j \sim \text{Normal}(\mu_j^{t0}, \sigma_j^{t0})$ where μ_j^{t0} was -2.10 and -2.13 for males and female respectively, and σ_j^{t0} was set at 5 for both sexes.

A sensitivity analysis was conducted where the priors for t0 were constrained ($\sigma_j^{t0} = 0$), and made to be more informative around a mean of zero.

3.5 Joint prior

For each model considered in the model ensemble, the biological parameterisation was the result of a single random draw from the appropriate joint posterior for each model. This preserved the inherent parameter correlation and meant that more samples were drawn from the more probable portions of the parameter distributions. Reproductive potential in the stock assessment was defined as the product of the female maturity at length relationship and the sex ratio at length relationship where the parameters from each of those relationships came from the appropriate posterior distribution. In this way the joint posterior from the Bayesian analysis becomes the joint prior for the model ensemble.

4 Standardisation of CPUE indices

Operational longline data for the European Union (i.e. Spanish), Japanese, and Chinese Taipei fisheries were standardized using spatiotemporal delta-Generalized Linear Mixed Models (GLMMs) applied in the VAST modelling framework (Thorson, 2019) in order to produce quarterly indices of relative abundance for use in the stock assessment model. This analysis builds heavily on the work described by Ducharme-Barth and Vincent (2020), and readers are directed to that report for background information and analytical detail as they will only be briefly summarized in this report. The data-sets and methods are essentially unchanged from that previous work, with the key differences being that swordfish is the target species for this analysis rather than bigeye or yellowfin tuna, and the spatial scope of the analysis is limited to the south Pacific Ocean to match the assessment area.

Briefly, the data-cleaning, species clustering (target species proxy), and missing hooks-between floats (HBF) reconstruction was applied to the Japan and Chinese Taipei operational data (Ducharme-Barth and Vincent, 2020). Species cluster analysis of the DWFN operational longline data identified 3 broad clusters: 1) high yellowfin tuna catches, 2) high albacore tuna catches, and 3) high bigeye tuna catches (Fig. 2). Since the European Union longline fishery primarily targets swordfish, it was assumed that this was the primary targeting behavior and species clustering to infer target was not conducted. Furthermore, HBF information for the European Union longline fishery was unavailable so the Random Forest machine learning approach was unable to be applied to predict what missing hooks might be.

The same delta modelling approach (described below) was applied to all three fleets and assumes that predicted catch-rate of a species is made up of two separable components: a binomial component accounting for encounter probability, and a positive catch component accounting for the rate of positive catches conditioned on the species being encountered. For the positive catch component a continuous gamma distribution was used as the error structure where positive catch was defined as numbers caught per 100 hooks fished (per set) for the Japanese and Chinese Taipei indices. Positive catch was defined in terms of catch in metric tons per set for the Spanish fleet, given that catch in numbers was unavailable until recently. For years when both definitions of catch were available, the nominal CPUE indices show very similar trends indicating that fish capture size is fairly constant over time.

Models differed between fleets only in the covariates that were available for inclusion in the model. However, covariate availability was generally very poor and only HBF, species cluster, and vessel ID were considered as operational covariates. These covariates were included in the model when available either as fixed (HBF and species cluster) or random effects (vessel). If available, HBF (binned in 5 hook increments) was treated as a cubic spline, and interacted with species cluster. This interaction attempted to account for the possibility that the same values of HBF did not result in the same swordfish catchability, depending on the predominant "target" tuna species due to potential differences in other unobserved operational gear characteristics. Additionally, given the diurnal diving behavior and influence of lunar illumination on night time swimming depth, lunar phase was calculated for all observations and included as cubic spline catchability effect.

The spatiotemporal delta-GLMMs that were applied as a part of the VAST modelling framework were comprised of the binomial component:

$$y_i \sim \text{Bernoulli}(p_i)$$

$$\log\frac{p_i}{1-p_i} = \text{YrQtr}_i + \omega_1(\text{s}_i) + \phi_1(\text{s}_i, \text{t}_i) + \text{Q}_i + \text{V}_{RE,i} + \epsilon_1$$

and the positive component:

$$c_i \sim \text{Gamma}(\sigma^{-2}, \mu_i\sigma^2)$$

$$\log(\mu_i) = \text{YrQtr}_i + \omega_2(\text{s}_i) + \phi_2(\text{s}_i, \text{t}_i) + \text{Q}_i + \text{V}_{RE,i} + \epsilon_2$$

where ω is the spatial random effect, ϕ is the spatiotemporal random effect, Q are the catchability covariate effects and V_{RE} are the vessel random effects. These spatial, and spatiotemporal random effects are define by the assumed "knot" structure of the model which are given in the following section for each model. Generally speaking, more knots are better, provided that you have enough data to appropriately estimate them. However, the number of knots used in any given model is determined by computational capabilities and a natural trade-off exists between the number of time-steps in the model and the number of "feasible" knots.

From the aforementioned approach, a total of 11 CPUE indices were developed from 8 different 'final' models. These are described in more detail for each fishery. For each "final" VAST model, several other candidate models with different estimated fixed effects for the catchability covariates were explored. The final model was retained based on AIC model selection. All retained models were determined to have converged based on achieving a low final gradient ($< 1 \times 10^{-5}$) and positive definite hessian solution. Residual analysis was performed using probability-integrated-transform (PIT) residuals (see Vidal et al., 2021 for a good description of PIT-type residuals).

4.1 European Union

As in the previous assessment, a single index was defined for the Spanish longline fishery operating in region 2. This index was generated from operational logbook data from 2004 – 2019, where the main latitudinal band of fishing activity was located from 20°S to 45°S. Within this band, effort seemed to shift seasonally (eastwards in the Austral summer, westwards in the Austral winter; towards 40°S during the Austral autumn and towards 25° during the Austral spring). Logbook reported operational covariates are unavailable for this fishery which limited the standardization modeling. Only vessel as a random effect, and lunar phase as a cubic spline were considered. Two-hundred spatial knots were assumed for this model.

4.2 Japan

Six indices were defined for the Japanese longline fishery, where indices were split according to time period and model region. Follow-up investigation of the operational longline data including summaries of operational setting characteristics from the Japanese observer program, as well as discussion with Japanese scientists led to the determination of the following three temporal periods: early (1952 – 1974), middle (1975 – 1993), and late (1994 – 2019). Several factors influenced the choice of these model periods including: 1) changes in logbook reporting procedures that likely improved the quality of catch and effort data from 1975, 2) the transition in mainline material (likely impacting the relationship between hooks per basket and fishing depth) in the mid-1990s from kuralon rope to monofilament, and 3) indication from the observer program data summaries that fishing and targeting practices differed for the Japanese fleet between regions 1 and 2. To account for these temporal and spatial splits, four separate VAST standardization models were applied to the Japanese operational longline data to generate the indices.

4.2.1 Early

Regions 1 and 2 were modelled together for the early time period since there was no information available to infer if catchability differences would exist between these regions. This model assumed 250 spatial knots and assumed the following covariate structures:

- Binomial: ∼ hooks fished + species cluster + s(lunar phase, d=3)
- Positive catch: ∼ species cluster + s(lunar phase, d=3)

HBF and vessel ID were not available for the early period.

4.2.2 Middle

Regions 1 & 2 were modelled together for the early time period since there was no information available to infer if catchability differences would exist between these regions. This model assumed 250 spatial knots and assumed the following covariate structures:

- Binomial: ∼ hooks fished + species cluster + s(HBF, d=3) + s(lunar phase, d=3)
- Positive catch: ∼ species cluster + s(HBF, d=3) + s(lunar phase, d=3)

Vessel ID was not available for the middle period.

4.2.3 Late - Region 1

In the late period, where there was information from the observer data to infer catchability differences (longer buoy and branchlines in the eastern portion of the model region, likely implying deeper fishing depth), and so separate VAST models were used in regions 1 and 2. The model for region 1 assumed 59 spatial knots which is lower than utilised in previous models, but was specified to maintain knot density as the 250 knots for the full region model. This model assumed the following covariate structures:

- Binomial: ∼ hooks fished + species cluster × s(HBF, d=3) + s(lunar phase, d=3) + V_{RE}
- Positive catch: ∼ species cluster × s(HBF, d=3) + s(lunar phase, d=3) + V_{RE}

4.2.4 Late - Region 2

This model assumed 194 spatial knots and fit to only the data in region 2. The decrease to 194 knots was to keep the equivalent knot density as the 250 knot full region model. This model assumed the following covariate structures:

- Binomial: ∼ hooks fished + species cluster × s(HBF, d=3) + s(lunar phase, d=3) + V_{RE}
- Positive catch: ∼ species cluster × s(HBF, d=3) + s(lunar phase, d=3) + V_{RE}

4.3 Chinese Taipei

Four indices were defined for the Chinese Taipei longline fishery. Similar to Japan, examination of the operational logbook data indicated apparent differences in targeting, based on observed catch composition, between regions 1 and 2 that could not be standardized out due to a lack of operational gear covariates. Additionally, the switch in mainline material during the 1990s was believed to be universal across all longline fisheries, though the exact timing of the change is uncertain. Accordingly, to account for this and a perceived shift towards bigeye tuna targeting in region 2, the index was split into two time periods for both regions: early (1965 – 1997), and late (1998 – 2019). To account for these temporal and spatial splits, three separate VAST standardization models were applied to the Chinese Taipei operational longline data to generate the indices.

4.3.1 Early

Regions 1 and 2 were modelled together for the early time period since there was no information available to infer if catchability differences would exist between these regions. This model assumed 250 spatial knots and assumed the following covariate structures:

- Binomial: ∼ hooks fished + species cluster × s(HBF, degree = 3) + s(lunar phase, degree = 3) + V_{RE}
- Positive catch: ∼ species cluster × s(HBF, degree = 3) + s(lunar phase, degree = 3) + V_{RE}

4.3.2 Late - Region 1

In the late period, where there was indication of a species composition change to more bigeye catches in region 2, a separate VAST model was used in each of regions 1 and 2. This model assumed 59 spatial knots and was fit to only the data in region 1. This model assumed the following covariate structures:

- Binomial: $\sim$ hooks fished + species cluster $\times$ s(HBF, degree = 3) + s(lunar phase, degree = 3) + V_{RE}
- Positive catch: $\sim$ species cluster $\times$ s(HBF, degree = 3) + s(lunar phase, degree = 3) + V_{RE}

4.3.3 Late - Region 2

This model assumed 194 spatial knots and was fit to only the data in region 2. This model assumed the following covariate structures:

- Binomial: $\sim$ hooks fished + species cluster $\times$ s(HBF, degree = 3) + s(lunar phase, degree = 3) + V_{RE}
- Positive catch: $\sim$ species cluster $\times$ s(HBF, degree = 3) + s(lunar phase, degree = 3) + V_{RE}

4.4 Results and discussion

The summaries of each of the CPUE standardisation models above are displyed in Fig. 3–9. These show the pattern of residuals by spatial knot, and the nominal and standardised CPUE indices. The model fit dignostics were adequate for all models and we consider the modelling process more robust than the previous analyses undertaken in 2017.

Some general comments are made on a case-by-case basis for each of the fisheries and models for which standardisations were undertaken:

- **EU index:** This fishery largely operates in the 20–40°S latitudinal band northeast of New Zealand (Fig. 3) and showed spatial patterns of CPUE that were variable through time, with highest CPUE pehaps concentrated adjacent to the New Zeland EEZ, and in the eastern extremeties of the region. The nominal and standardised indices were very similar with gentle long-term fluctuations that included periods of higher CPUE around 2005–2007 and 2015–2017, and lower CPUE around 2008–2011. There was substantial short term variation around these patterns.
- **Early JP index:** This fishery was regionally extensive and showed highest CPUE in the Tasman Sea (Fig. 4). The standardised indices for both regions displayed a steady increase in CPUE over the time period with very high seasonal variation, particularly in region 1. The standardised and nominal indices were similar with the most notable difference in both regions being higher CPUE in the first several years for the former.
- **Middle JP index:** Similar spatial patterns to the early period were observed (Fig. 5), although the nominal and standardised indices were relatively stable over this period in both regions, although with considerable seasonal variation, particulatly in region 1. The standardisation had little impact in region 1, aside from dampening the seasonal fluctuations in the most recent years. In region 2 the most notable impact of standardisation was the higher predicted CPUE in the early years.
- **Late JP R1 index:** The highest CPUE for this fishery occurred in the 25–40°S latitudinal band (Fig. 6). The resulting standardised index was high and variable in the first few years, declined to a lower level through the period 2000–2010, increased somewhat over 2010–2016 and then declined moderately in the final few years.
- **Late JP R2 index:** This fishery displayed very high CPUE in the northeast equatorial region (Fig. 7) and the standardised index showed a steady increase in CPUE over the full

time period, with high seasonal variability in recent years and perhaps a declining trend in the last few years.

- **Late TW R1 index:** Two patches of concentrated high CPUE were observed for this fishery - in the equatorial band, and another in the far south between about 20–30°S (Fig. 8). The standardised and nominal indices showed significant differences with the standardisation lowering and raising predicted CPUE in different periods, and removing some of the more pronounced extreme CPUE values evident in the nominal index. The resulting standardised index showed a general dome shape with CPUE peaking in the middle years of the index.
- **Late TW R2 index:** A similar spatial pattern to the late JP fishery was observed, where there were very high predicted CPUE values in the northeast equatorial region, particularly in the most recent years (Fig. 9). The standardised index showed a steady increasing trend, with substantial seasonal variation, especially in the last five years. There was perhaps a slight decline in CPUE in the last couple of years.

5 Preparation of size frequency data

5.1 Introduction

This section describes the reweighting of size composition data prior to integration into the 2021 southwest Pacific swordfish stock assessment model. Statistical correction of size composition data is undertaken as length and weight samples are often collected unevenly in space and time such that the samples require reweighting using either catch, to be representative of the size of fish being removed from the population in the case of extraction fisheries, or estimates of relative abundance, to be representative of the size of fish in the population in the case of index fisheries.

5.2 Methods

Swordfish size samples from longline fisheries were extracted from SPC's LF MASTER and WT MASTER databases, along with aggregate longline catch data from SPC's L BEST database. Size samples and aggregate catch data were matched, and aggregated, to consistent flag-fleet groupings using lookup tables provided by SPC's Data Management team. The size samples and aggregate catch data were also aggregated to a year-quarter temporal resolution to match the structure of the assessment model.

The procedure used to reweight the size compositions was based on that used to prepare bigeye and yellowfin size compositions for the 2020 assessments (Peatman et al., 2020), which itself was developed from the approach of McKechnie (2014) and Tremblay-Boyer et al. (2018) for regular and index fisheries respectively. The reweighting procedure was implemented at a $10 \times 20°$ spatial resolution. However, $10 \times 20°$ cells can span multiple assessment regions, as well as the boundary of the spatial domain of the assessment model. As an initial step, size samples were aggregated to a $10 \times 20°$ and region spatial resolution as follows:

- All size samples were split to a 5° spatial resolution using the proportion of reported catches by 5° degree cell for a given year-quarter and flag-fleet. For example, size samples provided at a $10 \times 20°$ resolution would be split between a maximum of eight 5° cells.
- The 5° cells were then assigned to an assessment model region, and any 5° cells outside the spatial domain of the assessment model were excluded.

- The size samples in each region were then aggregated back up to a $10 \times 20°$ and region spatial resolution, i.e. an overall resolution of year-quarter, region, $10 \times 20°$ cell and flag-fleet.

The size compositions were then reweighted spatially by fishery in the assessment model using the following approach:

- For a given fishery, size samples and aggregate catches (numbers) were aggregated to a stratification of year-quarter and $10 \times 20°$ cell.
- Size data from strata with fewer than 30 samples were excluded.
- 'Strata weights' for regular fisheries were then calculated using the proportion of catch over a time-window of $2k + 1$ quarters accounted for by each $10 \times 20°$ cell

$$W_{i,t} = \frac{\sum_{\tau=t-k}^{t+k} C_{i,\tau}}{\sum_i \sum_{\tau=t-k}^{t+k} C_{i,\tau}} \tag{1}$$

where $W_{i,t}$ and $C_{i,t}$ are the strata weight and catch (respectively) for $10 \times 20°$ cell i and year-quarter t. Strata weights for index fisheries were equivalent but weighted by estimated relative abundance from the CPUE standardisation model by $10 \times 20°$ cell and year-quarter, rather than catch.

- Strata-level numbers by size-class were then converted to proportions by size-class.
- Strata-level proportions by size-class were then weighted by multiplying by the appropriate strata weight $W_{i,t}$.
- The weighted proportions by size-class were then summed across strata to obtain proportions by size-class and year-quarter for the fishery.
- The fishery-resolution proportions by size-class were then raised to numbers by size-class, by multiplying by the total number of size samples for the fishery and year-quarter.

This approach implicitly scales the effective sample size at a fishery and year-quarter resolution by the proportion of catch (regular fisheries) or relative abundance (index fisheries) accounted for by $10 \times 20°$ cells with size samples. For example, if sampled $10 \times 20°$ cells accounted for 75% of the total catch for a fishery and year-quarter, then the effective sample size would be equal to 75% of the total sample size for that year-quarter. The fishery-resolution length compositions were then filtered for year-quarters where sampled $10 \times 20°$ cells accounted for a minimum proportion of the total catch of the fishery (regular fishery) or the total relative abundance in the corresponding assessment model region (index fisheries), i.e. filtering for year-quarters where the sum of strata weights from sampled $10 \times 20°$ cells exceeded a specified threshold. These minimum proportions are referred to throughout as the '''minimum sampled weighting'.

Effective samples were then rescaled appropriately for use with the different likelihood components used to model size compositions in MFCL, i.e. the robust-normal likelihood, and the self-scaling multinomial (SSM) likelihood. As described above, the reweighting procedure decreases effective sample sizes using the proportion of total catch (extraction fisheries) or abundance (index fisheries) from strata with length samples. Effective sample sizes for the robust-normal likelihood were then set at 50% of the down-weighted effective sample size when using index fisheries in the assessment model, to account for the use of the same length samples when generating length compositions for both index and regular fisheries. The effective sample sizes are then commonly scaled down further within MFCL as part of the model fitting process, typically by a factor in the range of 10 to 200. Effective sample sizes for the self-scaling multinomial likelihood were set at the original sample size, and again reduced by 50% if necessary as per sample sizes for the robust-normal likelihood. It is important to note that, whilst the effective sample sizes for the robust-normal and self-scaling multinomial can (and usually do) differ, the size compositions in proportional terms are the same.

There are both length and weight samples for southwest Pacific swordfish in SPC data holdings. There was a general preference to reweight both length and weight compositions where available given the relatively low numbers, and coverage, of size samples for swordfish compared to tropical tunas and albacore. However, only weight compositions were used for the Australian fishery in region 1, given that the weight samples are considered to be more representative than length samples for this fishery.

In common with other datasets, the reweighted compositions were insensitive to the length of the time-window used to calculate strata weights (e.g. Vidal et al., 2021). As such, we used time-windows consistent with those for 2021 albacore assessment (Vidal et al., 2021), i.e. a time-window of 11 quarters ($k = 5$) for extraction fisheries, and a time-window of 1 quarter ($k = 0$) for index fisheries.

A number of options were considered for distant water fishing nation (DWFN) extraction fisheries: using samples from vessels flagged to Japan; using samples from vessels flagged to Japan, Korea and China; and, using all available samples from DWFN flag-fleets. Initial reweighting runs indicated that the reweighted compositions were insensitive to the various sub-sets of flag-fleets in terms of the resulting size distributions and their temporal variation. However, excluding samples from flag-fleets did reduce the number of year-quarters with available data. As such, we used samples from all DWFN flag-fleets when generating size compositions for DWFN extraction fisheries.

5.3 Results and discussion

The reweighting of size compositions for this year's southwest Pacific swordfish assessment is a new development, with unweighted compositions used in the 2017 assessment (Takeuchi et al., 2017). Comparisons of reweighted and raw compositions indicated that the reweighting procedure reduced noise in the size compositions, through both the exclusion of data from strata with limited samples, and the exclusion of data from year-quarters with limited sampling coverage. However, there was still appreciable levels of apparent noise in reweighted size compositions, particularly for time-periods and fisheries with limited samples (Figs. 10–19).

The choice of minimum sampled weighting is a compromise between attempting to remove temporal variation in sizes as a result of limited and unbalanced sampling, whilst attempting to minimise filtering of size compositions and so preserve temporal coverage of reweighted compositions (e.g. McKechnie, 2014). Threshold values of 0.3 and 0.1 have been recommended for extraction and index fisheries respectively for recent assessments of tropical tunas and albacore (e.g. Peatman et al., 2020; Vidal et al., 2021). If possible, we would recommend that these thresholds also be used in the swordfish assessment. However, lower thresholds may need to be applied in order to estimate selectivity functions for all fisheries given the relatively low numbers of size samples. We recommend assessing the sensitivity of the assessment model to the minimum sampled weighting threshold, given that the selection of the threshold is subjective and somewhat arbitrary. Thresholds of 0.5 and 0.3 would be appropriate for extraction and index fisheries respectively for assessing sensitivity of the model to stronger data filtering, though again consideration of lower thresholds may be required.

Weight compositions were generated with both 10kg and 5kg size-classes. Comparisons of reweighted size compositions suggested that there was information at a 5kg resolution that was smoothed-over and potentially lost at a 10kg resolution. For example, the apparent cohort progression for sizes ranging from 12 to 32kg in 5kg weight compositions for the Australian extraction fishery in region 1 (Fig. 15) is difficult to discern (at least visually) at a 10kg resolution. As such, we recommend considering a move from 10kg to 5kg weight-classes.

There were sufficient length and weight samples for the New Zealand extraction fishery in region 2 to assess the consistency between the reweighted length and weight compositions. Length compositions were converted to units of weight, and vice versa, using the length-weight relationship $W = 1.347e^{-5} \times L^{2.997}$. The length and weight compositions were generally in agreement, though the weight compositions had larger fish in 2008, and generally exhibited more temporal variation, than length samples (Fig. 20). The time-series for length compositions was longer, though the number of length samples per year-quarter was lower than those for weight. The lack of conflict between the length and weight samples supports the inclusion of both length and weight compositions for the New Zealand extraction fishery in region 2. We did not attempt similar comparisons between length and weight compositions for other fisheries due to the relative paucity of weight samples, though conflict between length and weight compositions should be apparent in diagnostic plots.

Spatial stratification was used to reweight length compositions for both extraction and index fisheries, i.e. strata were defined as combinations of $10 \times 20°$ cell and year-quarter. This accounts for spatial variation in size compositions within a region, but does not account for any additional variation between flag-fleets. Ideally, stratification both spatially and by flag-fleet should be used for extraction fisheries, to account for both of these sources of variation. However, there was insufficient sampling coverage to implement more detailed stratification in the reweighting procedure for all extraction fisheries, noting that moving to a finer stratification increases the risk of introducing additional noise into time series of size compositions. We also note that, for extraction fisheries, stratification by flag-fleet gave comparable compositions to spatial stratification.

Acknowledgments

T. Peatman's contribution was supported by the European Union's "Pacific-European Union Marine Partnership Programme". We are also grateful for J. Farley at CSIRO who facilitated access to the biological data. Thanks also to T. Vidal and S. McKechnie who provided editorial contributions.

References

Castillo-Jordan, C., Xu, H., Hampton, J., Ducharme-Barth, N., and Hamer, P. (2021). Stock assessment of south pacific albacore. Technical Report WCPFC-SC17-2021/ST-WP-02, Electronic meeting, 11–19 August 2021.

Ducharme-Barth, N., Castillo-Jordan, C., Hampton, J., Hamer, P. Williams, P., and Pilling, G. (2021). Stock assessment of Southwest Pacific swordfish. Technical Report WCPFC-SC17-2021/SA-WP-04, Electronic meeting, 11–19 August 2021.

Ducharme-Barth, N. and Vincent, M. (2020). Analysis of Pacific-wide operational longline dataset for bigeye and yellowfin tuna catch-per-unit-effort (CPUE). Technical Report WCPFC-SC16-2020/SC16-SA-IP-07.

Ducharme-Barth, N. and Vincent, M. (2021). Focusing on the front end: A framework for incorporating uncertainty in biological parameters in model ensembles of integrated stock assessments. Technical Report WCPFC-SC17-2021/SA-WP-05, Electronic meeting, 11–19 August 2021.

Ducharme-Barth, N., Vincent, M., Hampton, J., Hamer, P., Williams, P., and Pilling, G. (2020). Stock assessment of bigeye tuna in the western and central Pacific Ocean. Technical Report WCPFC-SC16-2020/SA-WP-03 [REV3].

Farley, J., Clear, N., Kolody, D., Krusic-Golub, K., Eveson, P., and Young, J. (2016). Determination of swordfish growth and maturity relevant to the southwest Pacific stock. WCPFC-SC12-2016/SA-WP-11, Bali, Indonesia, 3–11 August 2016.

Farley, J., Krusic-Golub, K., Eveson, P., Clear, N., Roupsard, F., Sanchez, C., Nicol, S., and Hampton, J. (2020). Age and growth of yellowfin and bigeye tuna in the western and central Pacific Ocean from otoliths. Technical Report WCPFC-SC16-2020/SA-WP-02, Electronic meeting, 11–20 August 2020.

Hamer, P., Castillo Jordon, C., Xu, H., Ducharme-Barth, N., and Vidal Cunningham, T. (2021). Report from the SPC Pre-assessment Workshop - March 2021. Technical Report WCPFC-SC17-2021/SA-IP-02, Pacific Community.

McInturff, P., Johnson, W. O., Cowling, D., and Gardner, I. A. (2004). Modelling risk when binary outcomes are subject to error. *Statistics in Medicine*, 23(7):1095–1109.

McKechnie, S. (2014). Analysis of longline size frequency data for bigeye and yellowfin tunas in the WCPO. WCPFC-SC10-2014/SA-IP-04, Majuro, Republic of the Marshall Islands, 6–14 August 2014.

Peatman, T., Ducharme-Barth, N., and Vincent, M. (2020). Analysis of purse-seine and longline size frequency data for bigeye and yellowfin tuna in the WCPO. WCPFC-SC16-2020/SA-IP-18, Electronic meeting, 11–19 August 2020.

STAN Development Team (2021). Stan modeling language users guide and reference manual. https://mc-stan.org.

Takeuchi, Y., Pilling, G., and Hampton, J. (2017). Stock assessment of swordfish (*Xiphias gladius*) in the southwest Pacific Ocean. Technical Report WCPFC-SC13-2017/SA-WP-13, Rarotonga, Cook Islands, 9–17 August 2017.

Thorson, J. T. (2019). Guidance for decisions using the Vector Autoregressive Spatio-Temporal (VAST) package in stock, ecosystem, habitat and climate assessments. *Fisheries Research*, 210:143–161.

Tremblay-Boyer, L., Hampton, J., McKechnie, S., and Pilling, G. (2018). Stock assessment of South Pacific albacore tuna in the WCPO. Technical Report WCPFC-SC14-2021/SA-WP-05, Busan, Republic of Korea, 8–16 August 2018.

Vidal, T., Castillo Jordan, C., Peatman, T., Ducharme-Barth, N., Xu, H., Williams, P., and Hamer, P. (2021). Background analyses and data inputs for the 2021 South Pacific albacore tuna stock assessment. Technical Report WCPFC-SC17-2021/SA-IP-03.

Vincent, M., Ducharme-Barth, N., Hamer, P., Hampton, J., Williams, P., and Pilling, G. (2020). Stock assessment of yellowfin tuna in the western and central Pacific Ocean. WCPFC-SC16-2020/SA-WP-04-Rev2.

Young, J., Drake, A., Brickhill, M., Farley, J., and Carter, T. (2003). Reproductive dynamics of broadbill swordfish, *Xiphias gladius*, in the domestic longline fishery off eastern Australia. *Marine and Freshwater Research*, 54(4):1–18.

6 Figures

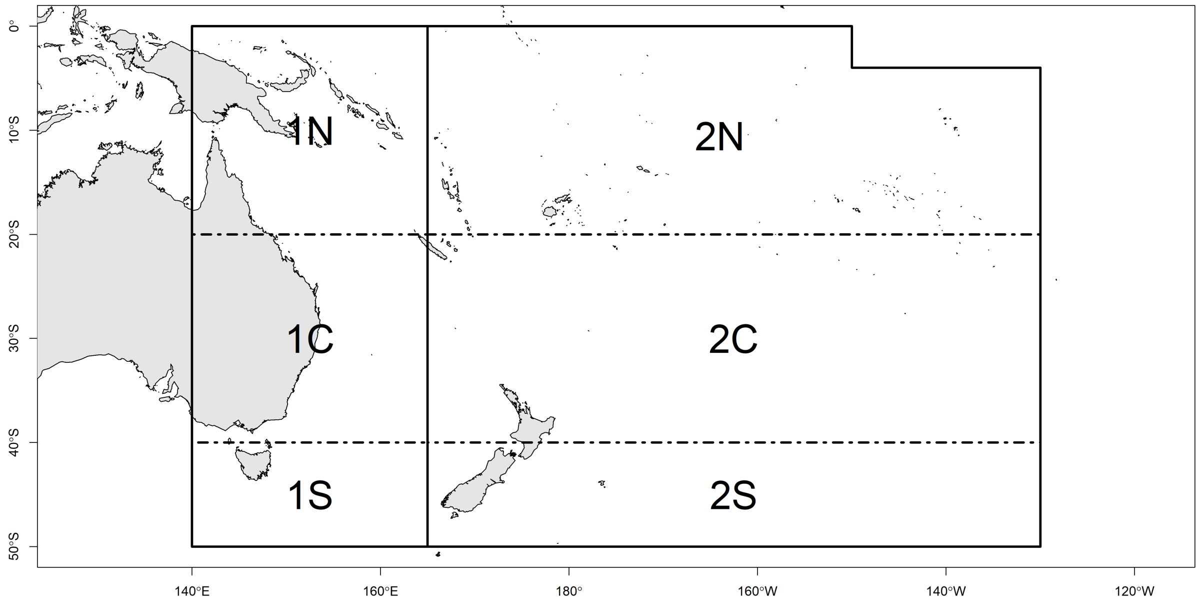

Figure 1: Spatial structure of the 2020 southwest Pacific swordfish stock assessment.

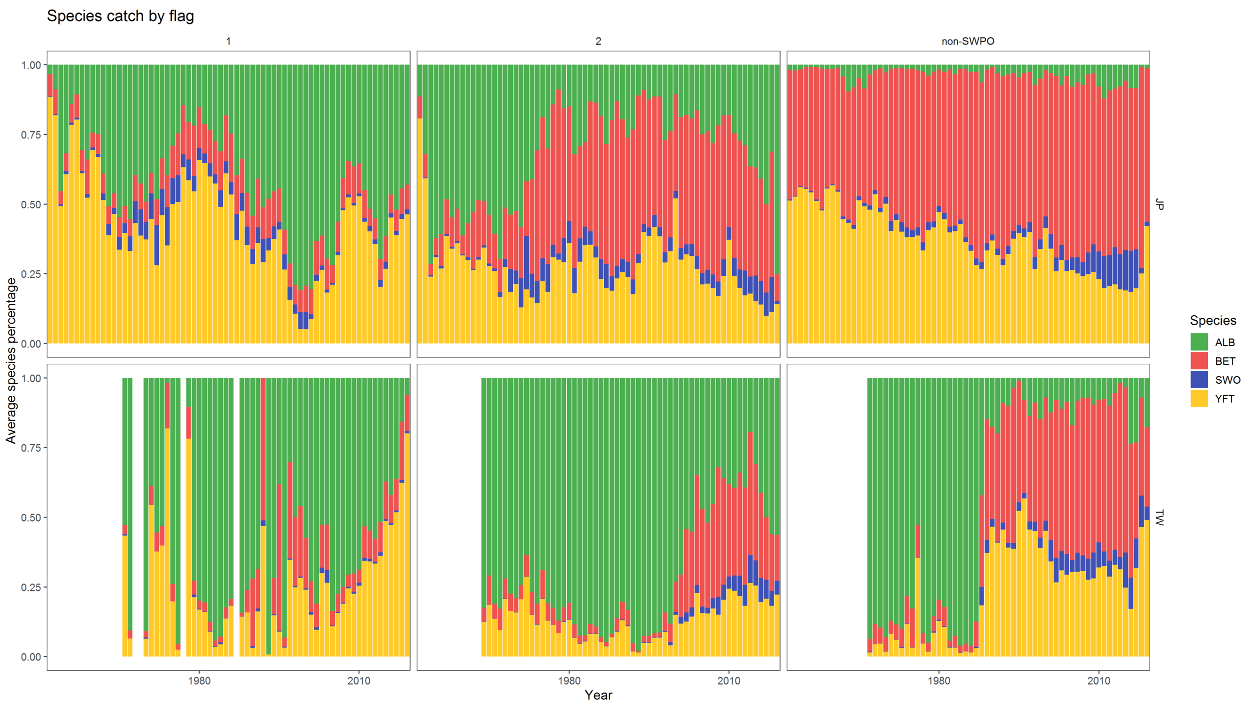

Figure 2: Catch proportions for the four main species (albacore, ALB; bigeye, BET; swordfish, SWO; yellowfin, YFT) for data from the operational logsheet database for Japan (top panels) and Chinese Taipei (bottom panels).

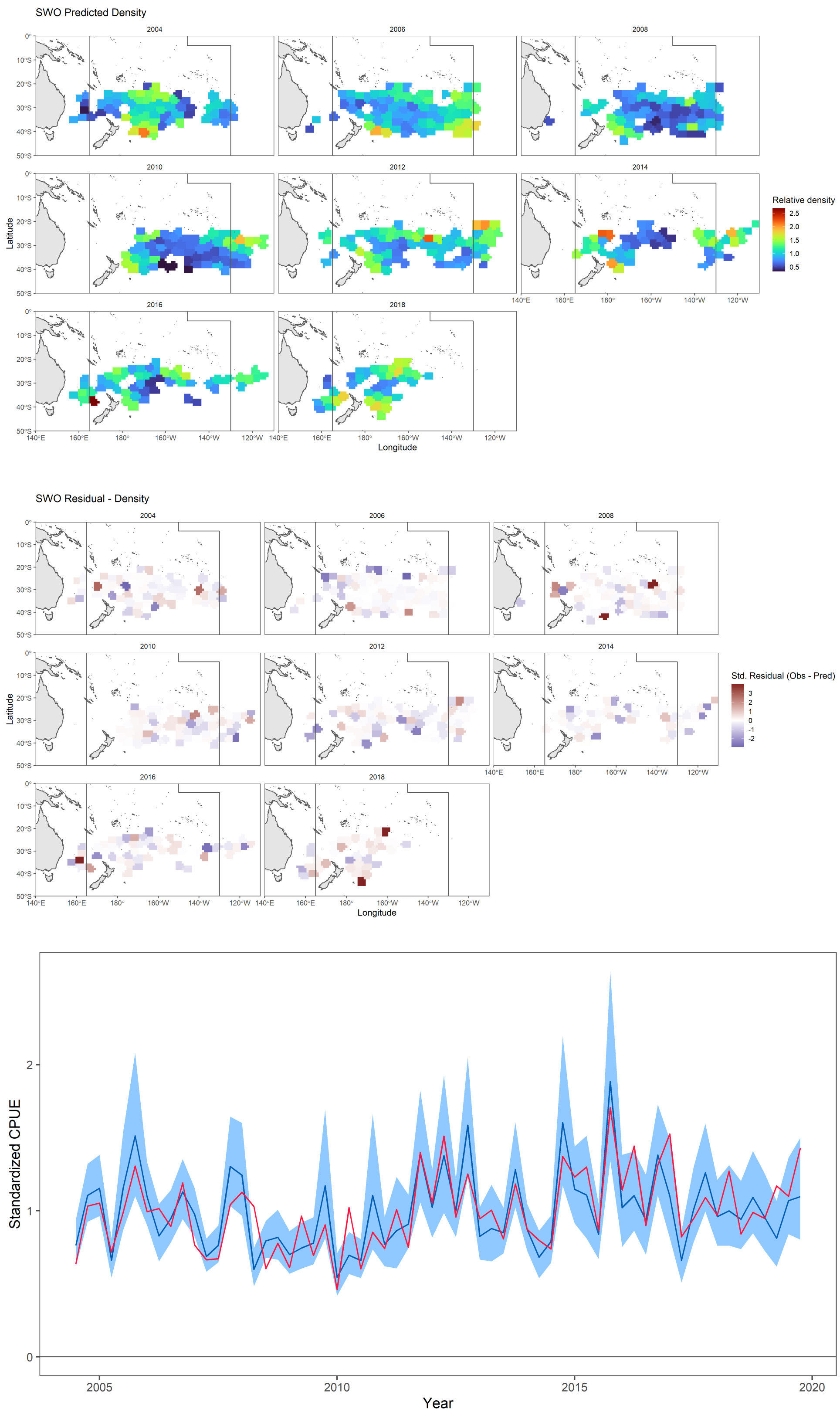

Figure 3: Summaries of CPUE standardisations for the EU fishery; predicted CPUE distributions (top), spatial patterns in residuals (middle), both displayed in 2-yearly blocks, and the resulting nominal (red line) and standardised (blue line, mean; blue ribbon, 95% CI) indices (bottom), both nomalised to have a mean of 1.

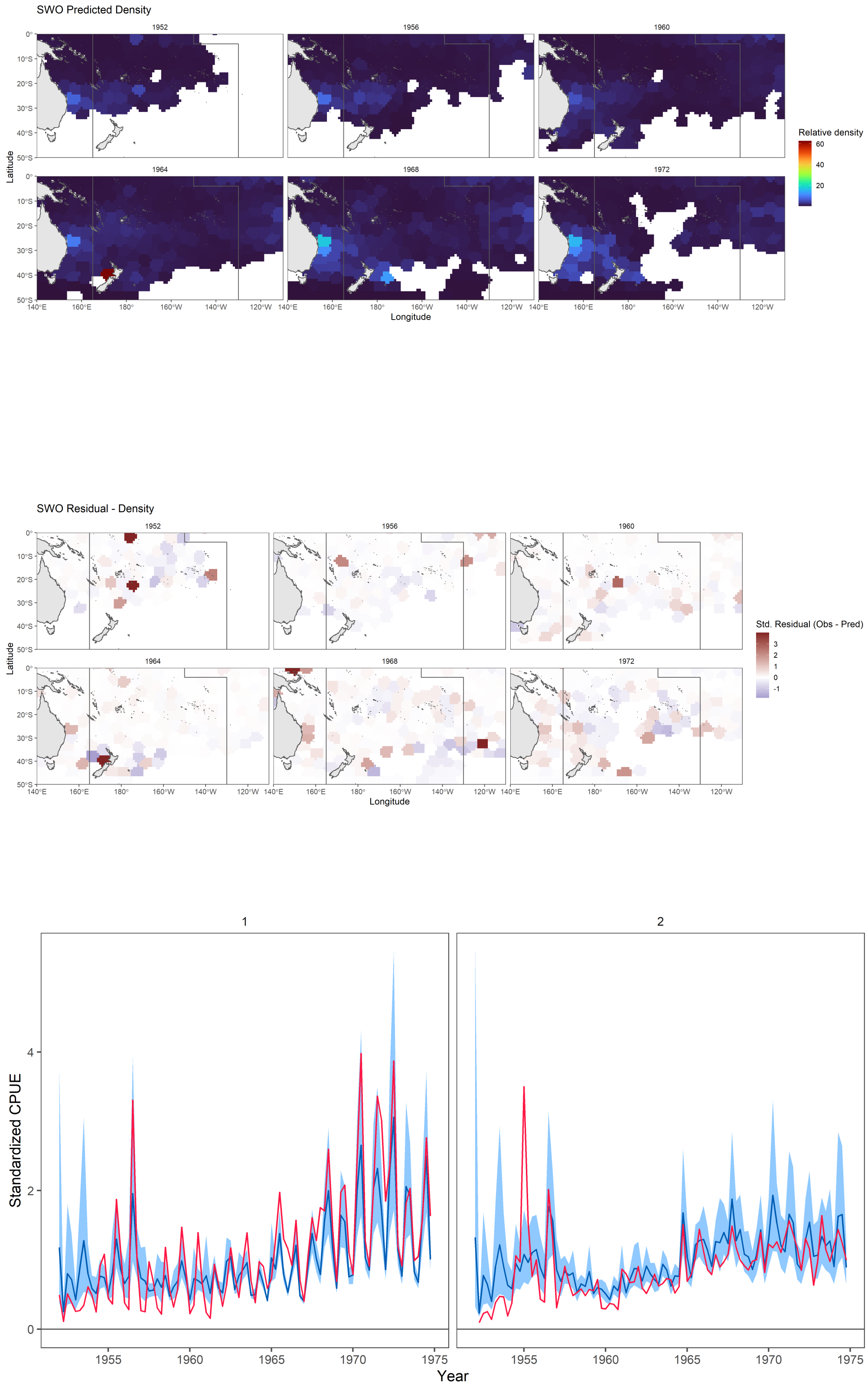

Figure 4: Summaries of CPUE standardisations for the early JP fishery (1952–1974).

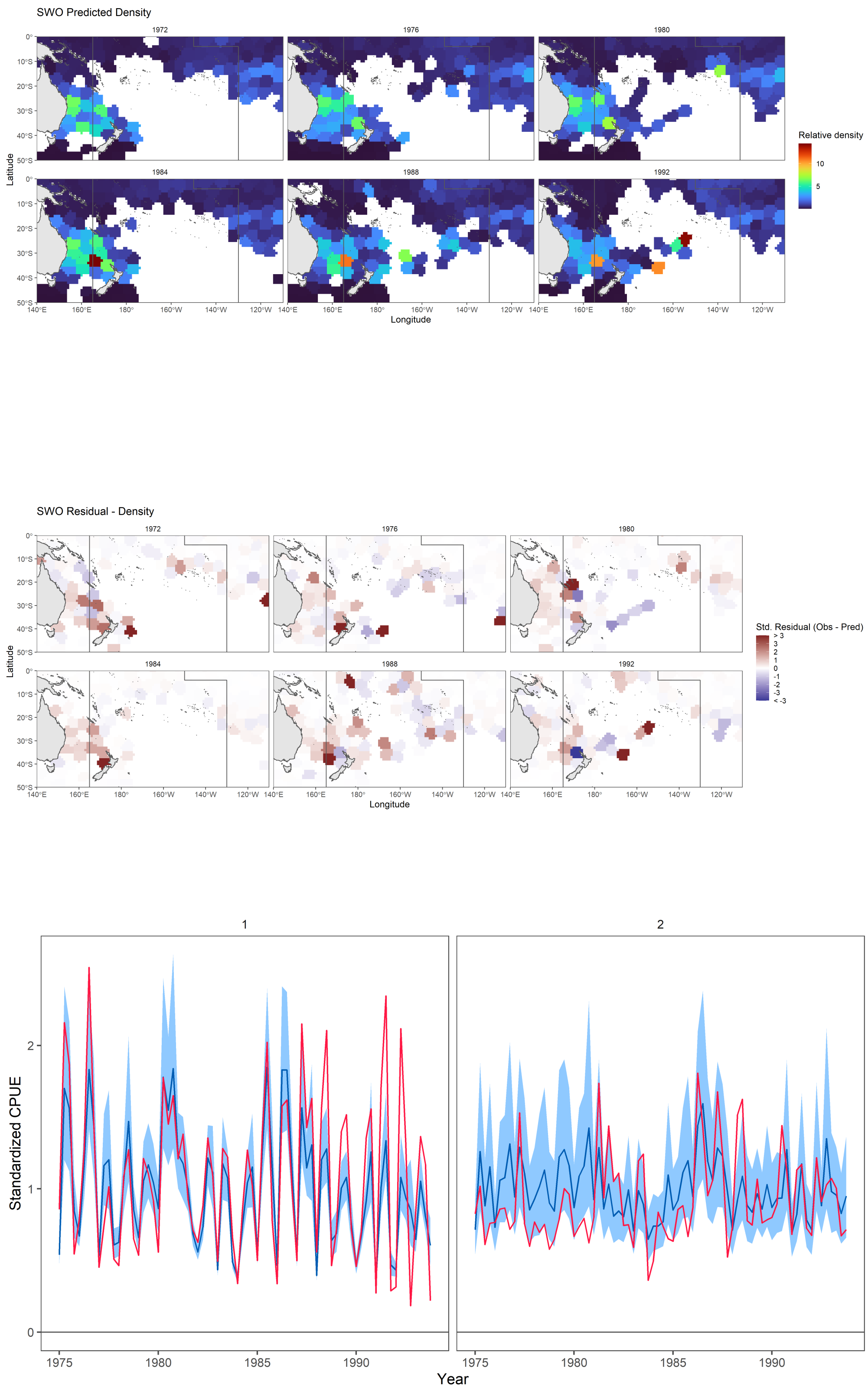

Figure 5: Summaries of CPUE standardisations for the middle years JP fishery (1975–1993).

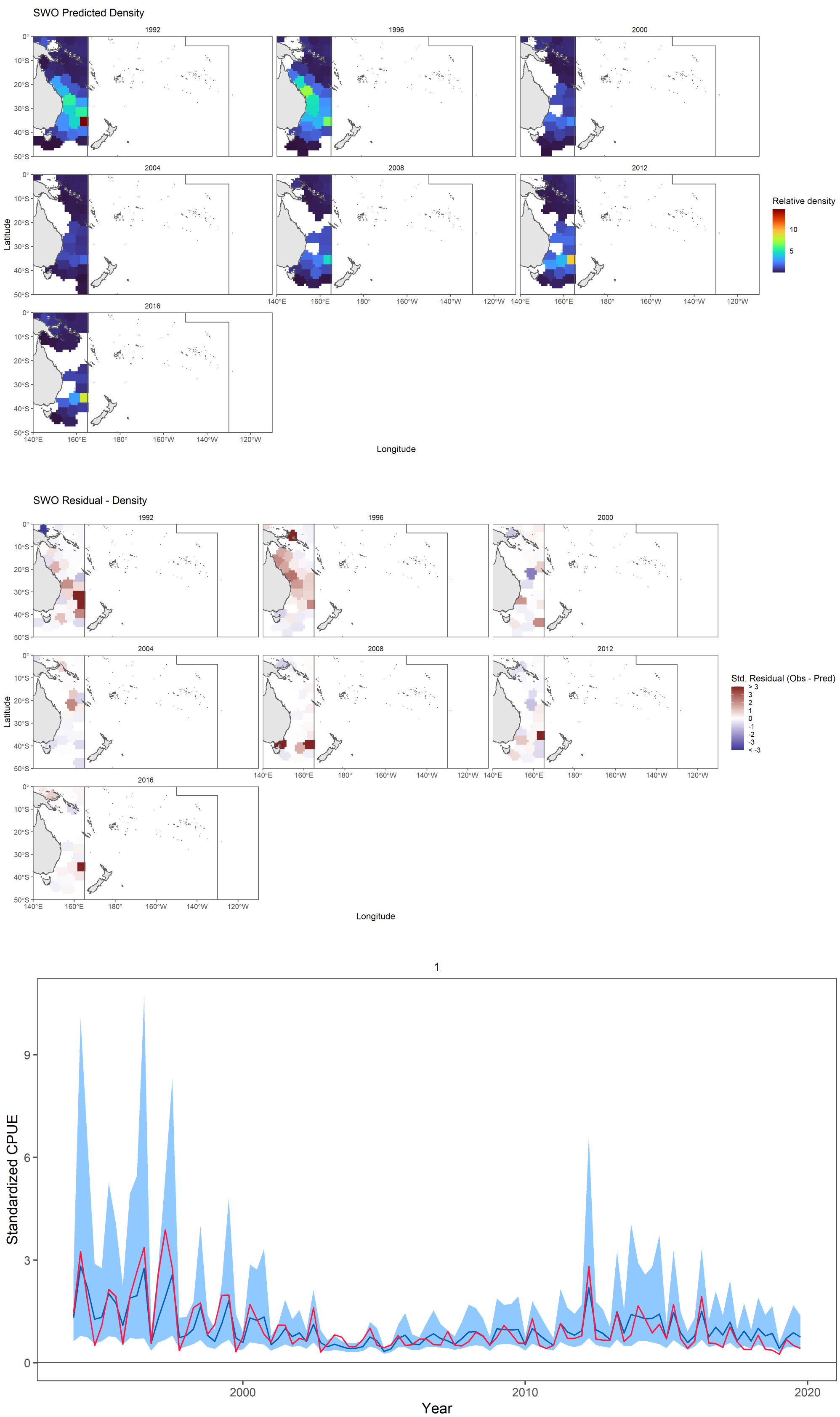

Figure 6: Summaries of CPUE standardisations for the late JP fishery in region 1 (1994–2019).

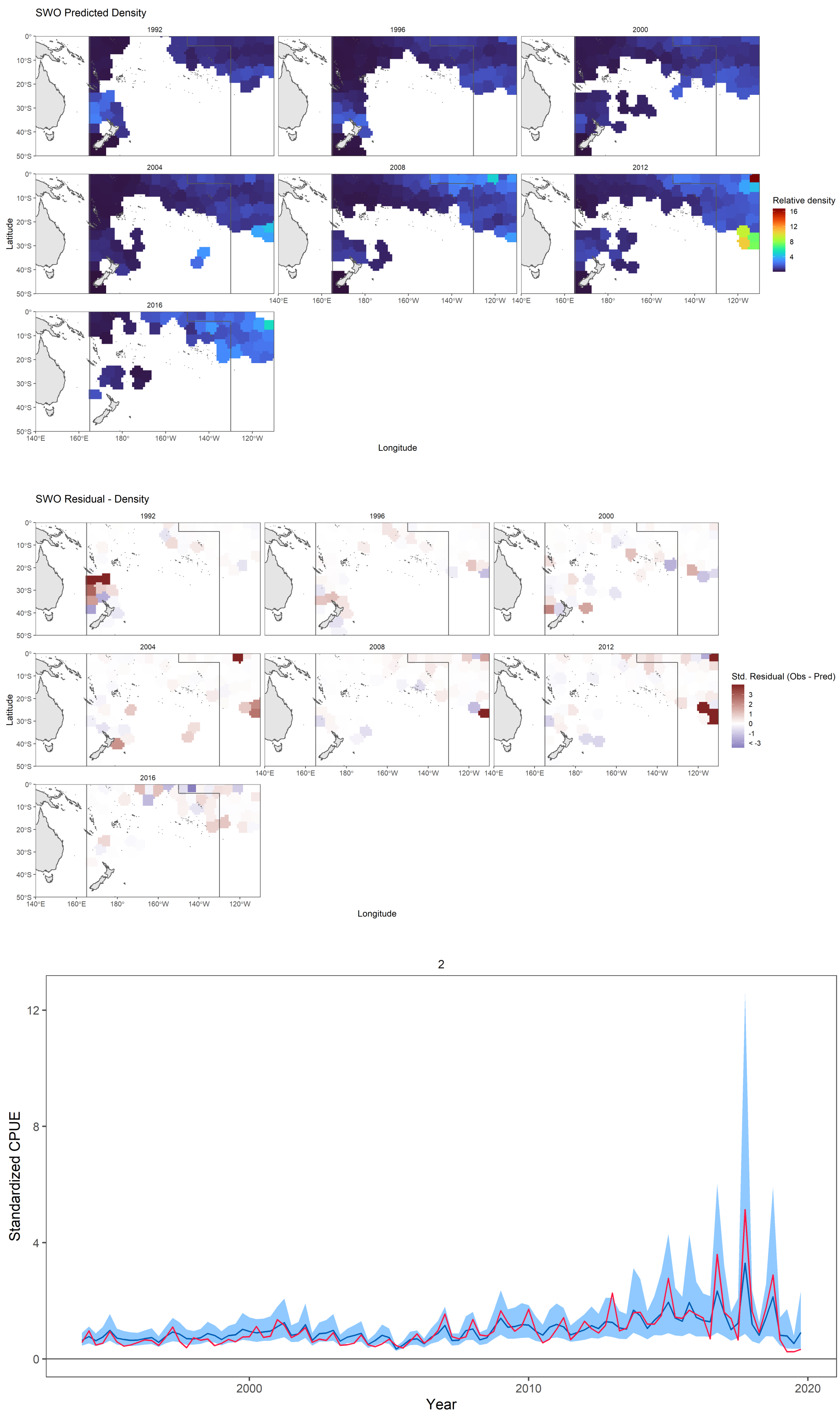

Figure 7: Summaries of CPUE standardisations for the late JP fishery in region 2 (1994–2019).

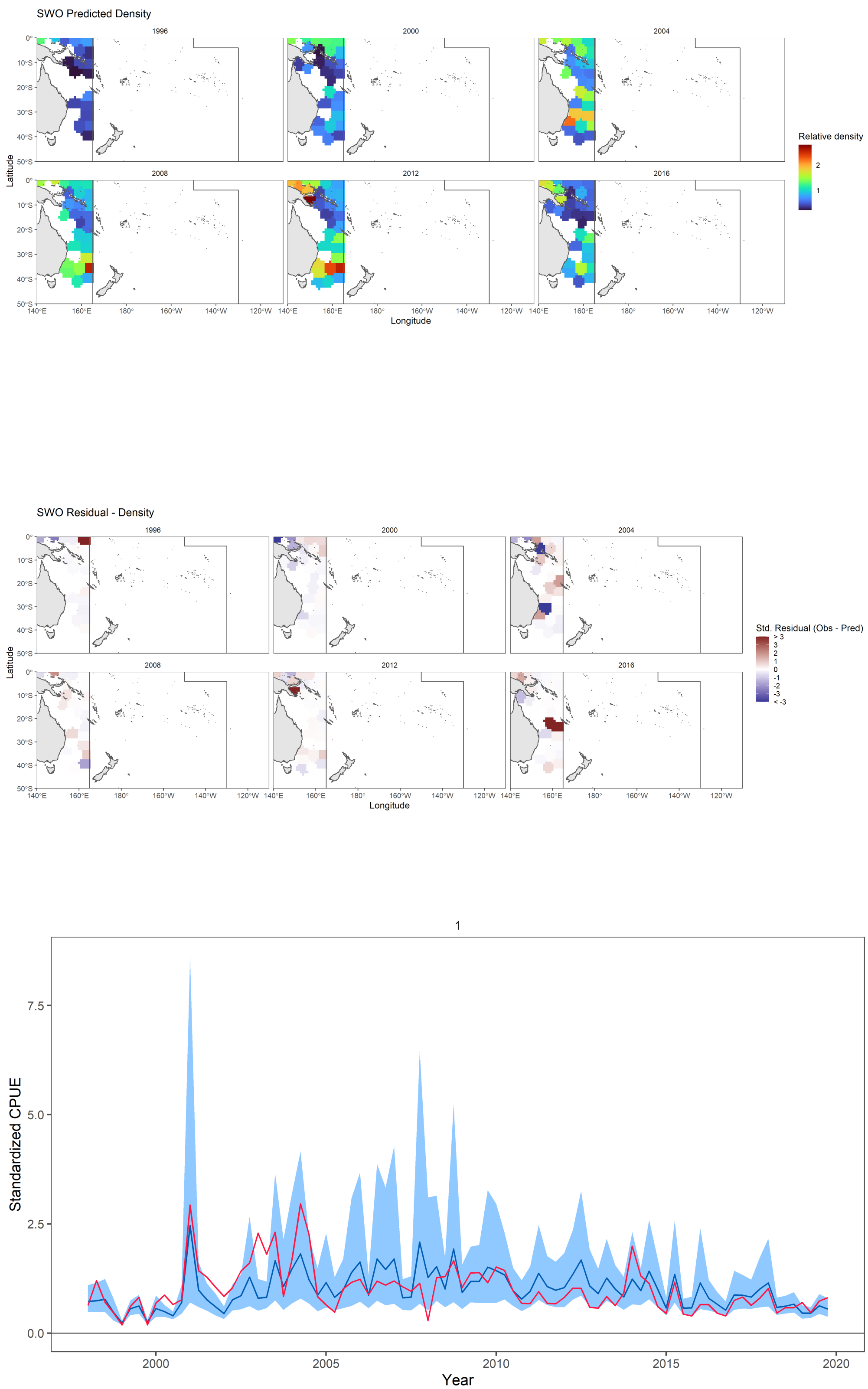

Figure 8: Summaries of CPUE standardisations for the late TW fishery in region 1 (1998–2019).

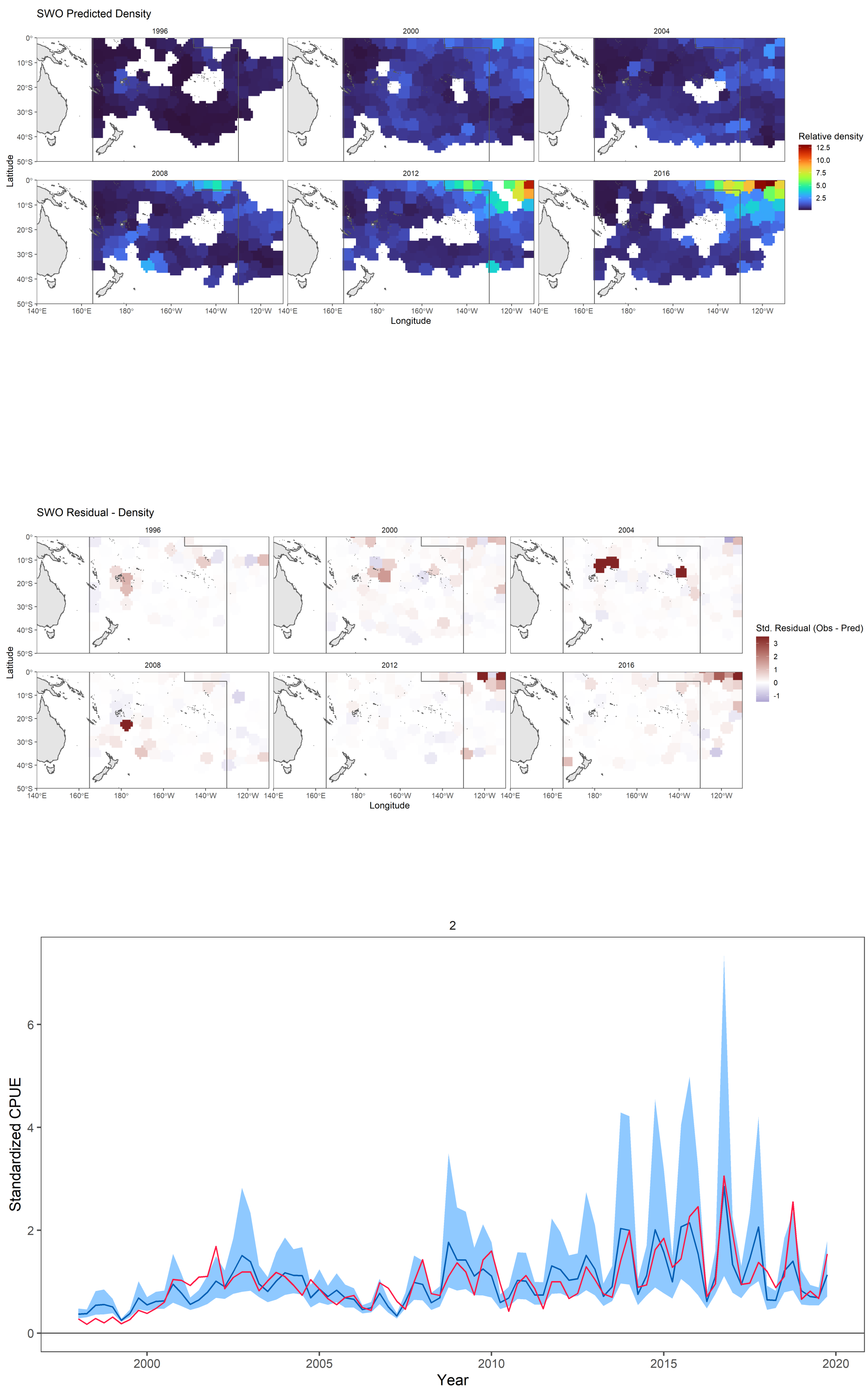

Figure 9: Summaries of CPUE standardisations for the late TW fishery in region 2 (1998–2019).

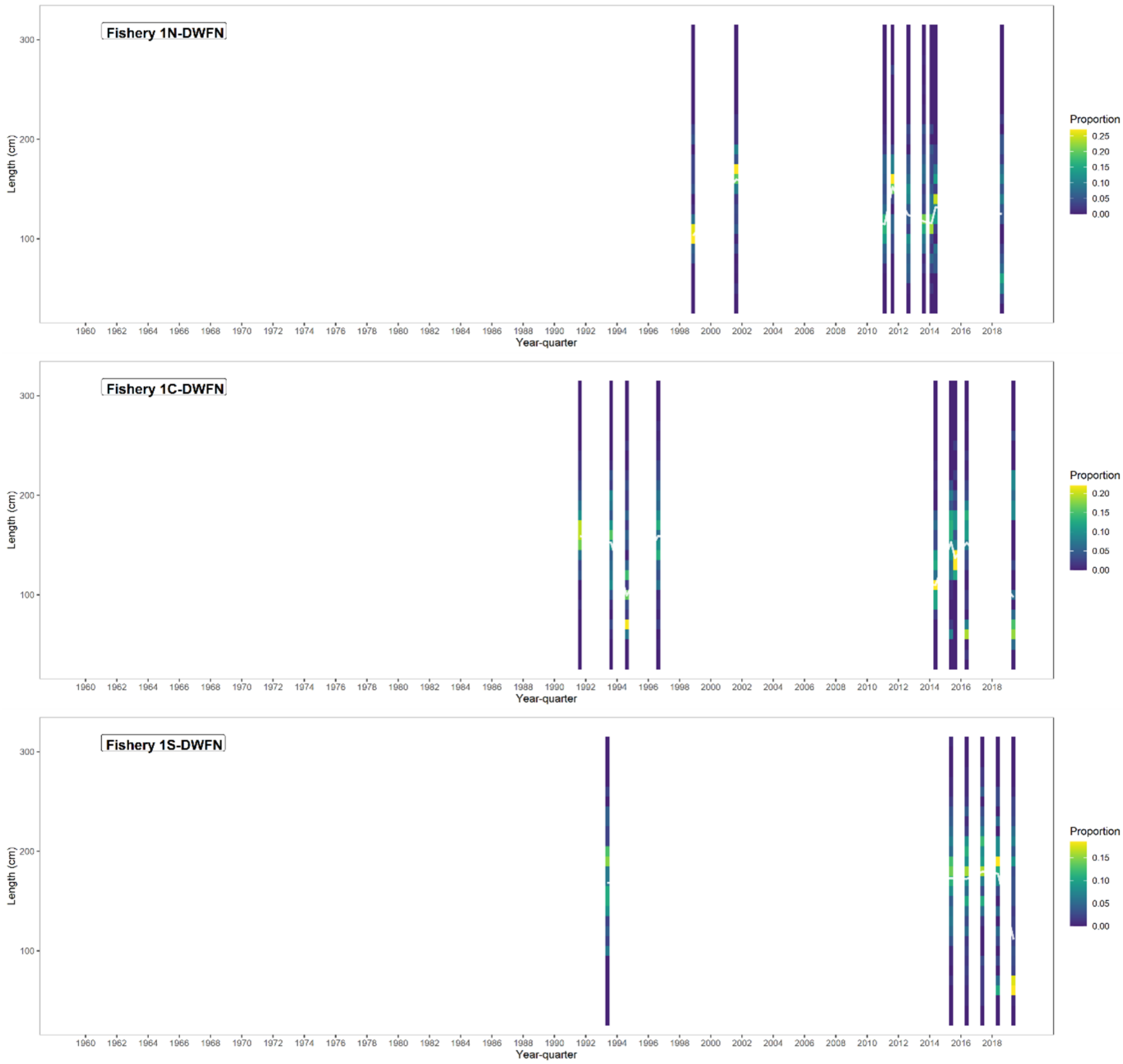

Figure 10: Reweighted length compositions for the distant water fishing nation (DWFN) extraction fisheries in region 1 north (top panel), region 1 central (middle) and region 1 south (bottom panel). The white line provides the median size by year-quarter. A minimum sampled weighting of 0.3 was applied.

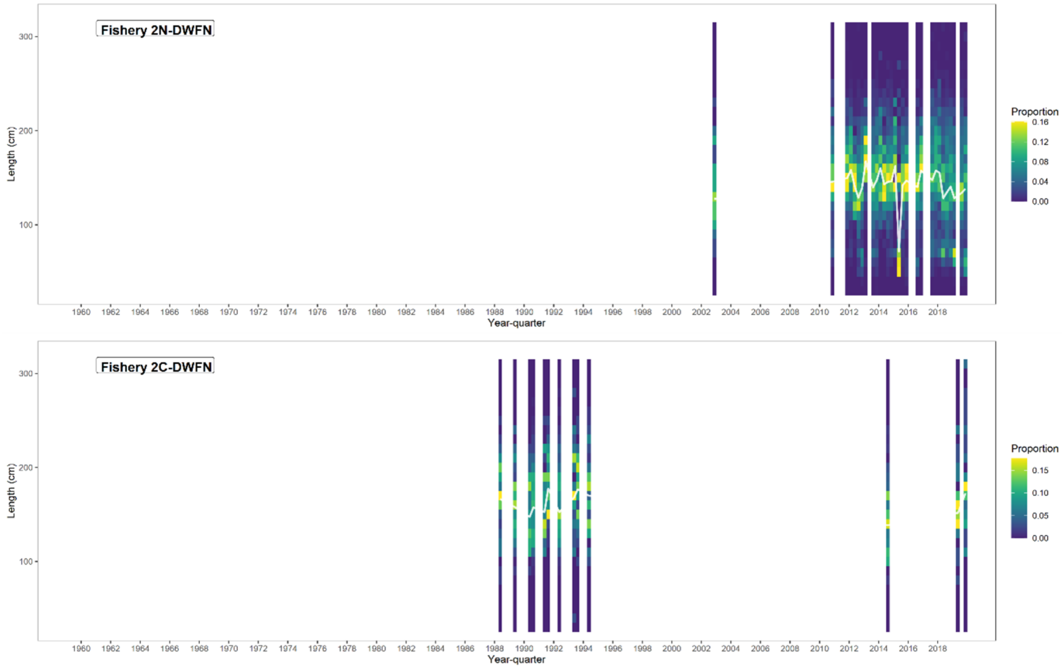

Figure 11: Reweighted length compositions for the distant water fishing nation (DWFN) extraction fisheries in region 2 north (top panel), and region 2 central (bottom panel). The white line provides the median size by year-quarter. A minimum sampled weighting of 0.3 was applied.

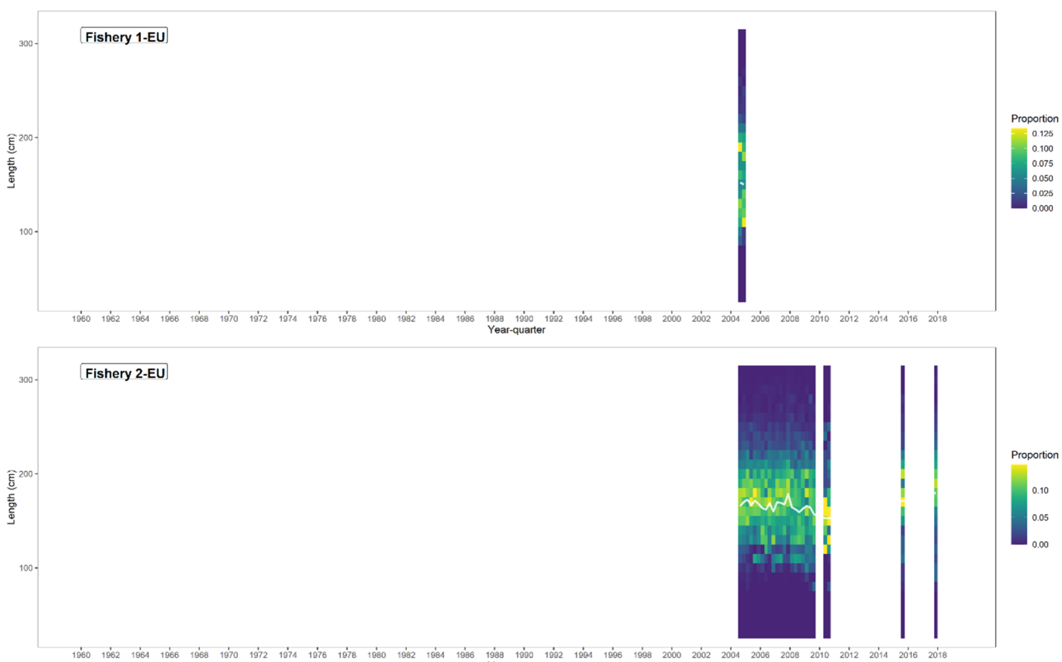

Figure 12: Reweighted length compositions for the EU extraction fishery in region 1 (top panel) and region 2 (bottom panel). The white line provides the median size by year-quarter. A minimum sampled weighting of 0.3 was applied.

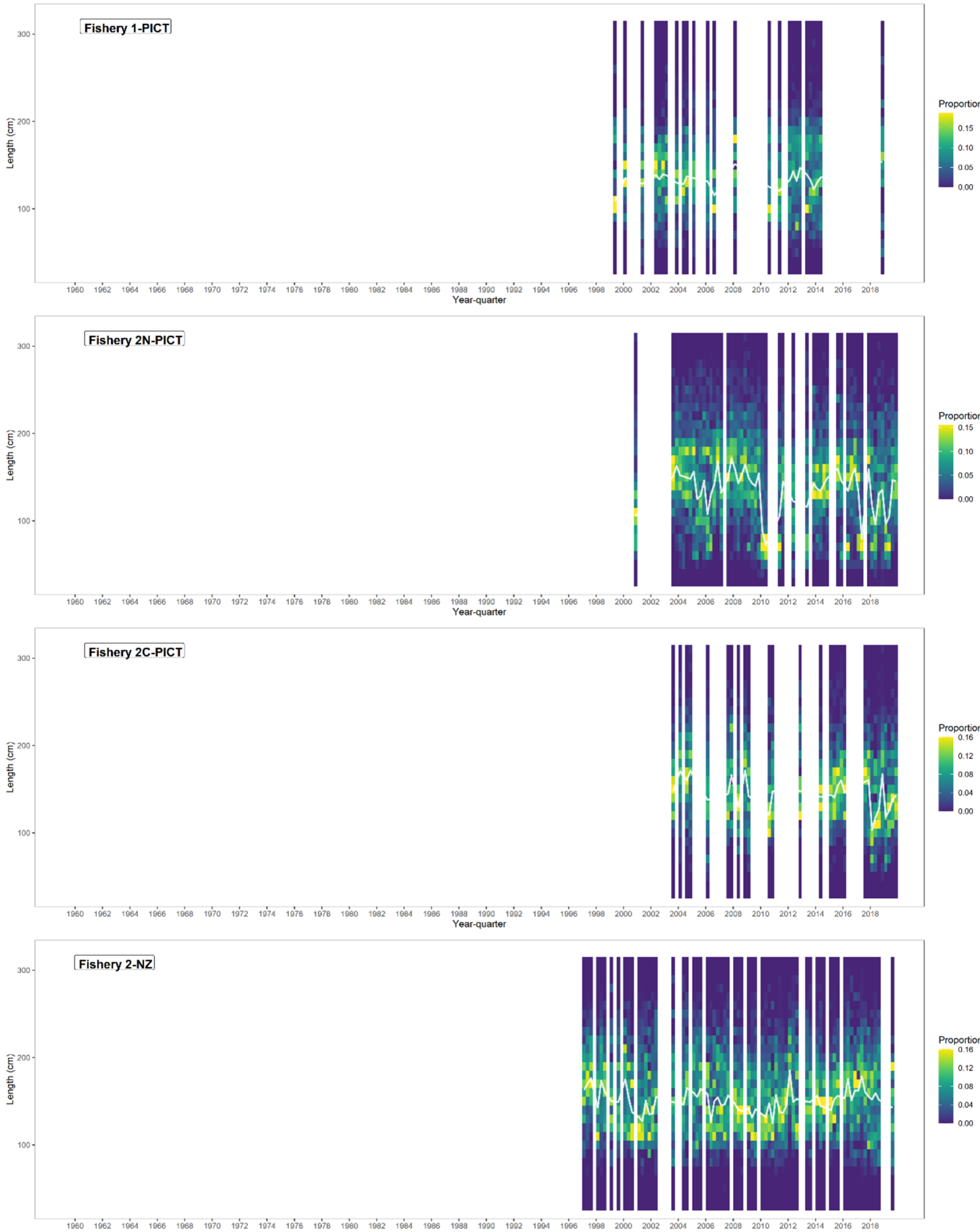

Figure 13: Reweighted length compositions for the Pacific Island Country and Territory (PICT) extraction fishery in region 1 (top panel), region 2 north (second panel) and region 2 south (third panel), and the New Zealand extraction fishery in region 2 (bottom panel). The white line provides the median size by year-quarter. A minimum sampled weighting of 0.3 was applied.

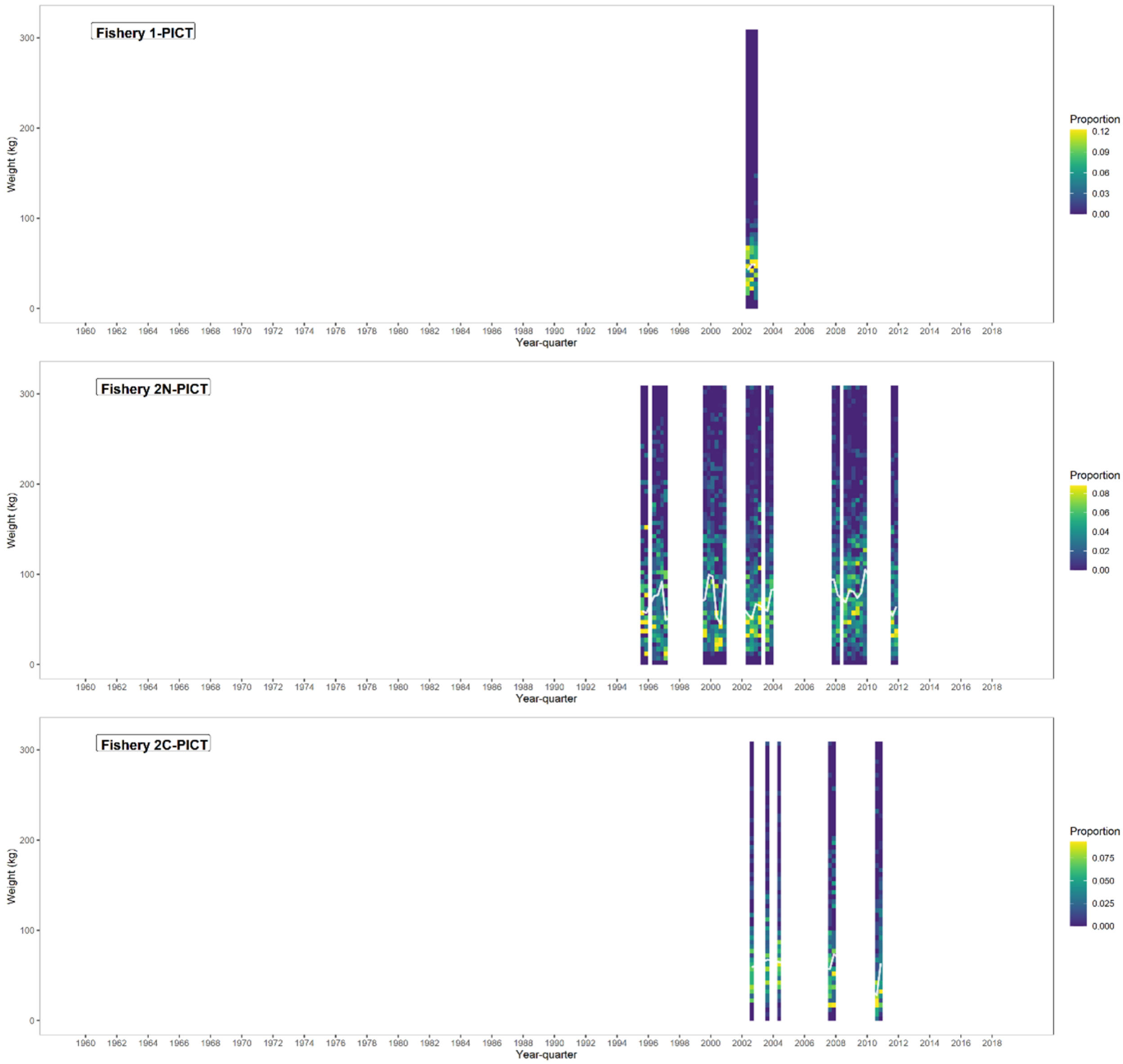

Figure 14: Reweighted weight compositions with 5kg weight-classes for the Pacific Island Country and Territory (PICT) extraction fishery in region 1 (top panel), region 2 north (middle) and region 2 central (bottom panel). The white line provides the median size by year-quarter. A minimum sampled weighting of 0.3 was applied.

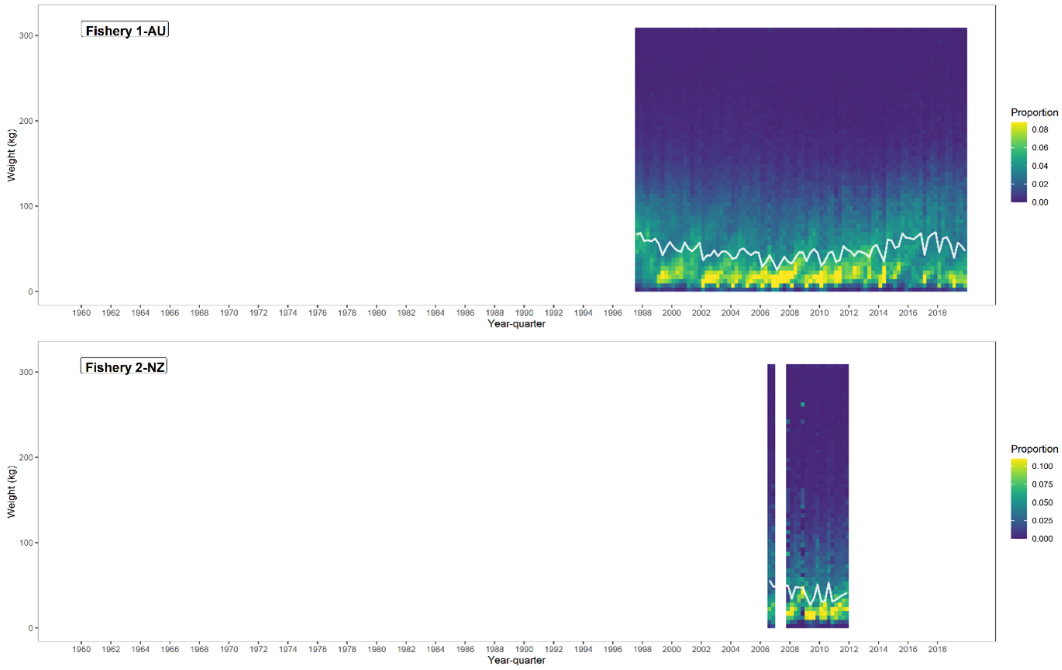

Figure 15: Reweighted weight compositions with 5kg weight-classes for the Australian extraction fishery in region 1 (top panel), and the New Zealand extraction fishery in region 2 (bottom panel). The white line provides the median size by year-quarter. A minimum sampled weighting of 0.3 was applied.

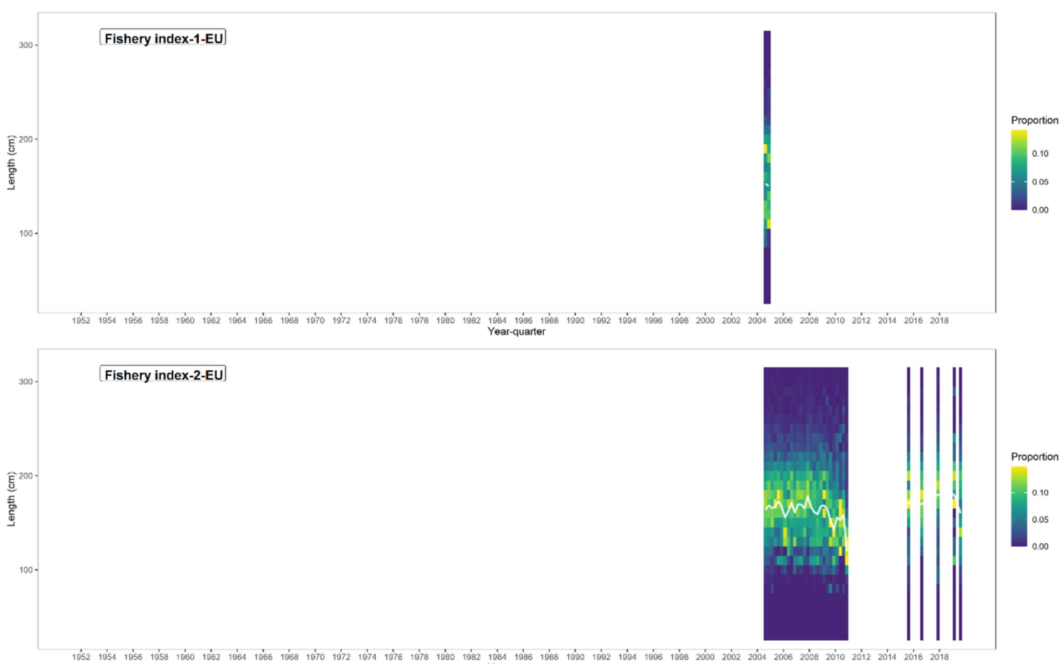

Figure 16: Reweighted length compositions for the EU index fishery in region 1 (top panel) and region 2 (bottom panel). The white line provides the median size by year-quarter. A minimum sampled weighting of 0.1 was applied.

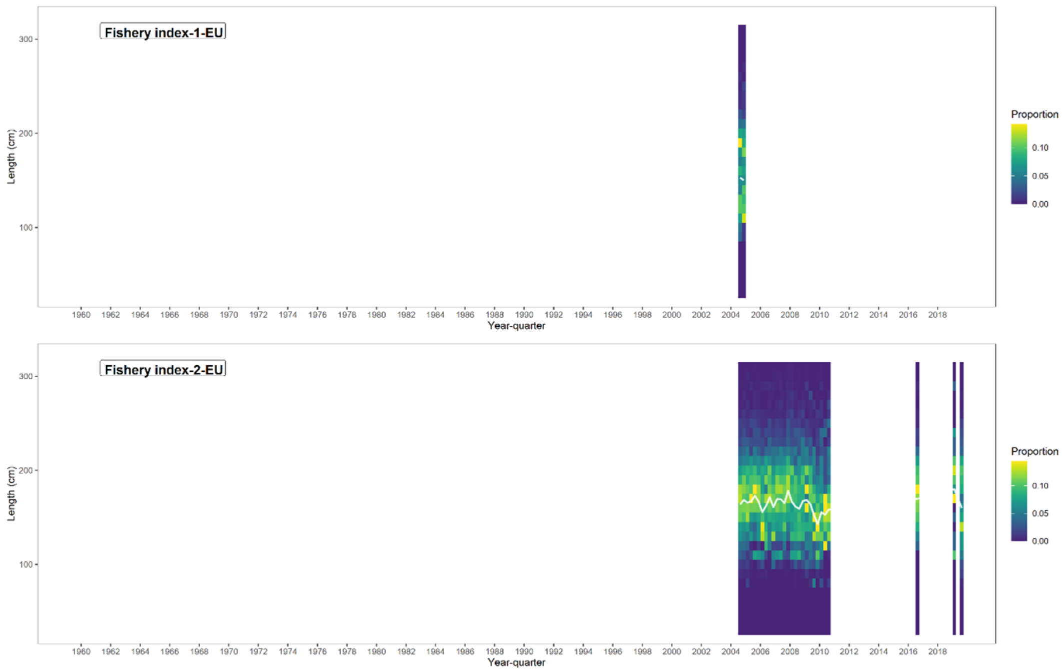

Figure 17: Reweighted length compositions for the EU index fishery in region 1 (top panel) and region 2 (bottom panel). The white line provides the median size by year-quarter. A minimum sampled weighting of 0.1 was applied.

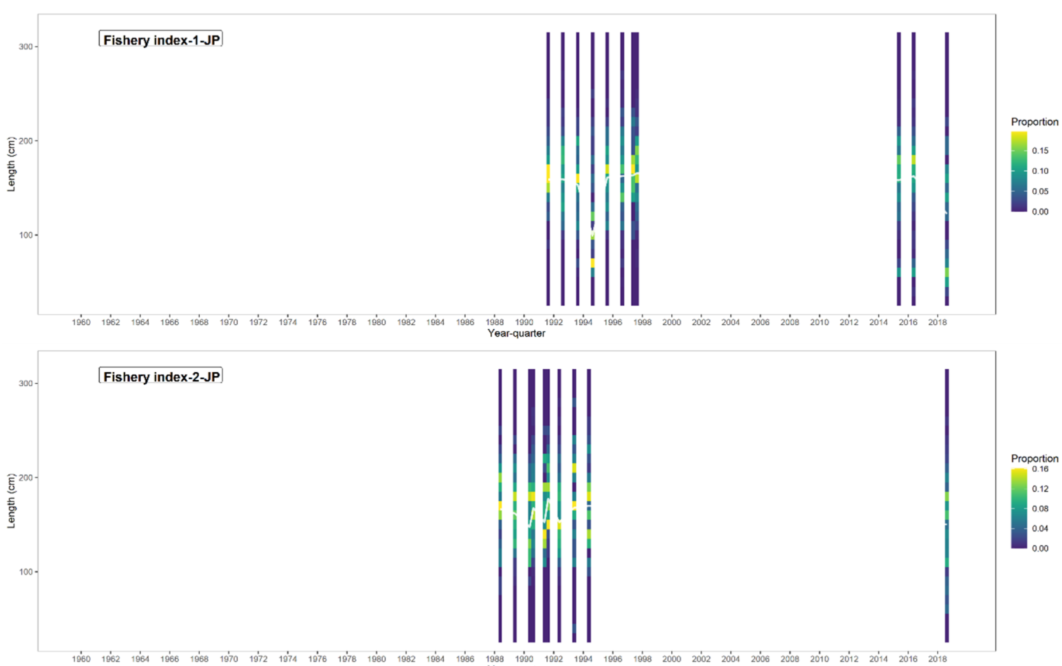

Figure 18: Reweighted length compositions for the Japan index fishery in region 1 (top panel) and region 2 (bottom panel). The white line provides the median size by year-quarter. A minimum sampled weighting of 0.1 was applied.

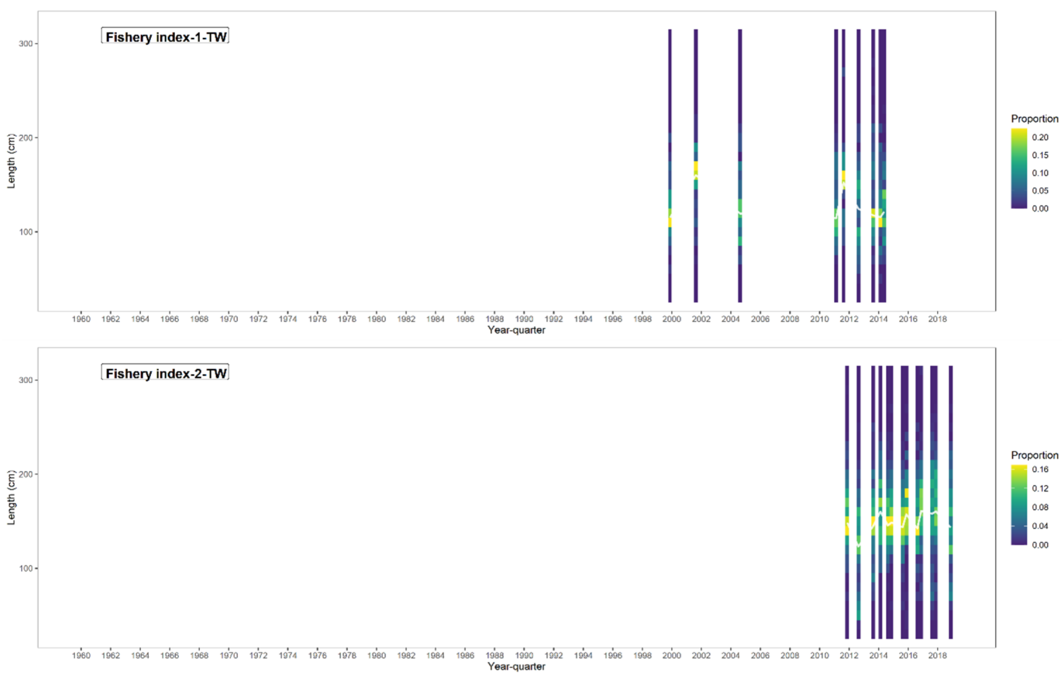

Figure 19: Reweighted length compositions for the Japan index fishery in region 1 (top panel) and region 2 (bottom panel). The white line provides the median size by year-quarter. A minimum sampled weighting of 0.1 was applied.

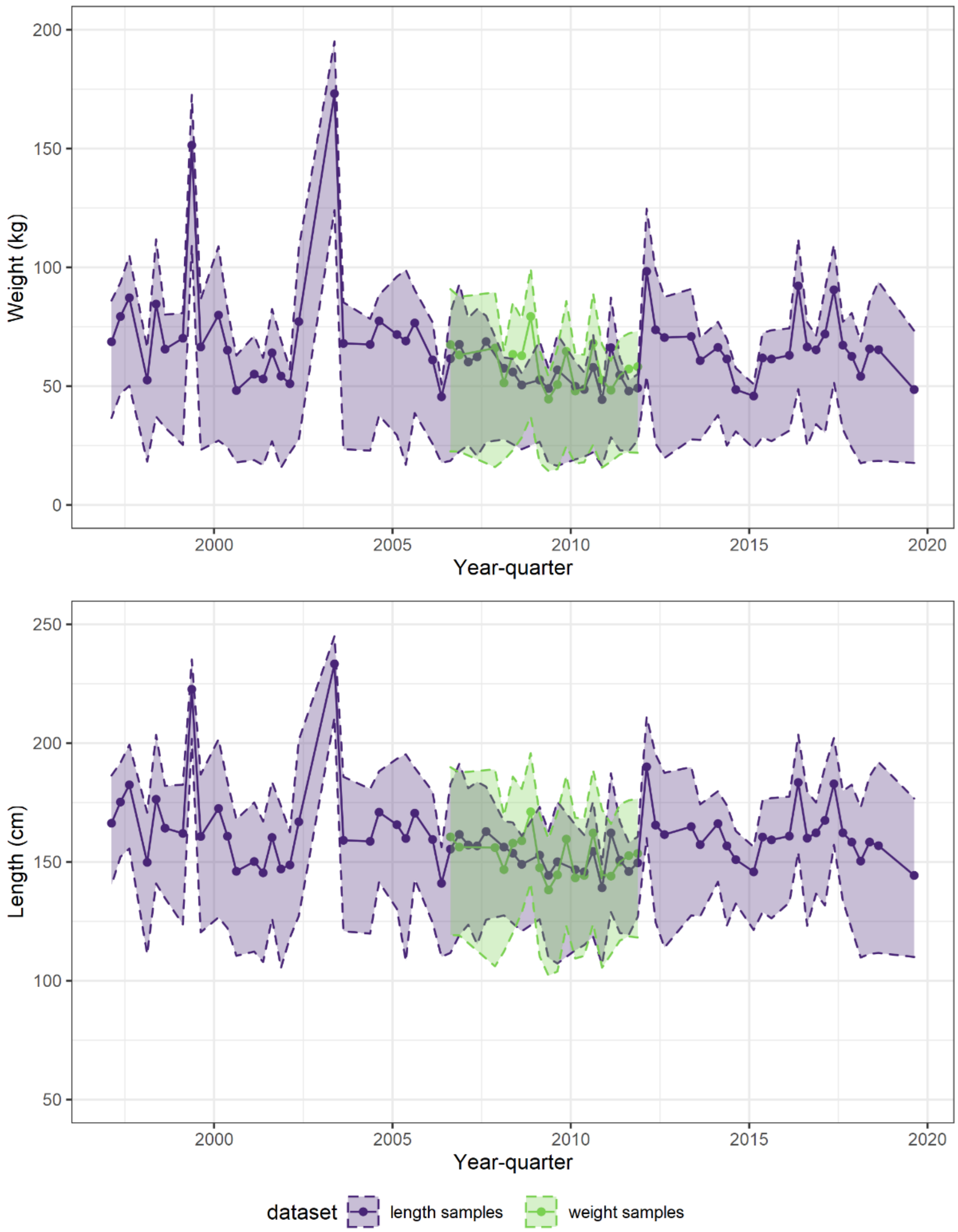

Figure 20: Comparisons of reweighted length (purple) and weight (green) compositions for the New Zealand fishery in region 2. The solid line and points are the mean size, and the dashed line and ribbon is the inter-quartile range. The top panel compares weight compositions against the length compositions, having converted the length compositions into units of weight (see text). The bottom panel compares the length compositions against the weight compositions, having converted the weight compositions into units of length.

Appendix 1: Summary plots of fisheries definitions used in the stock assessment

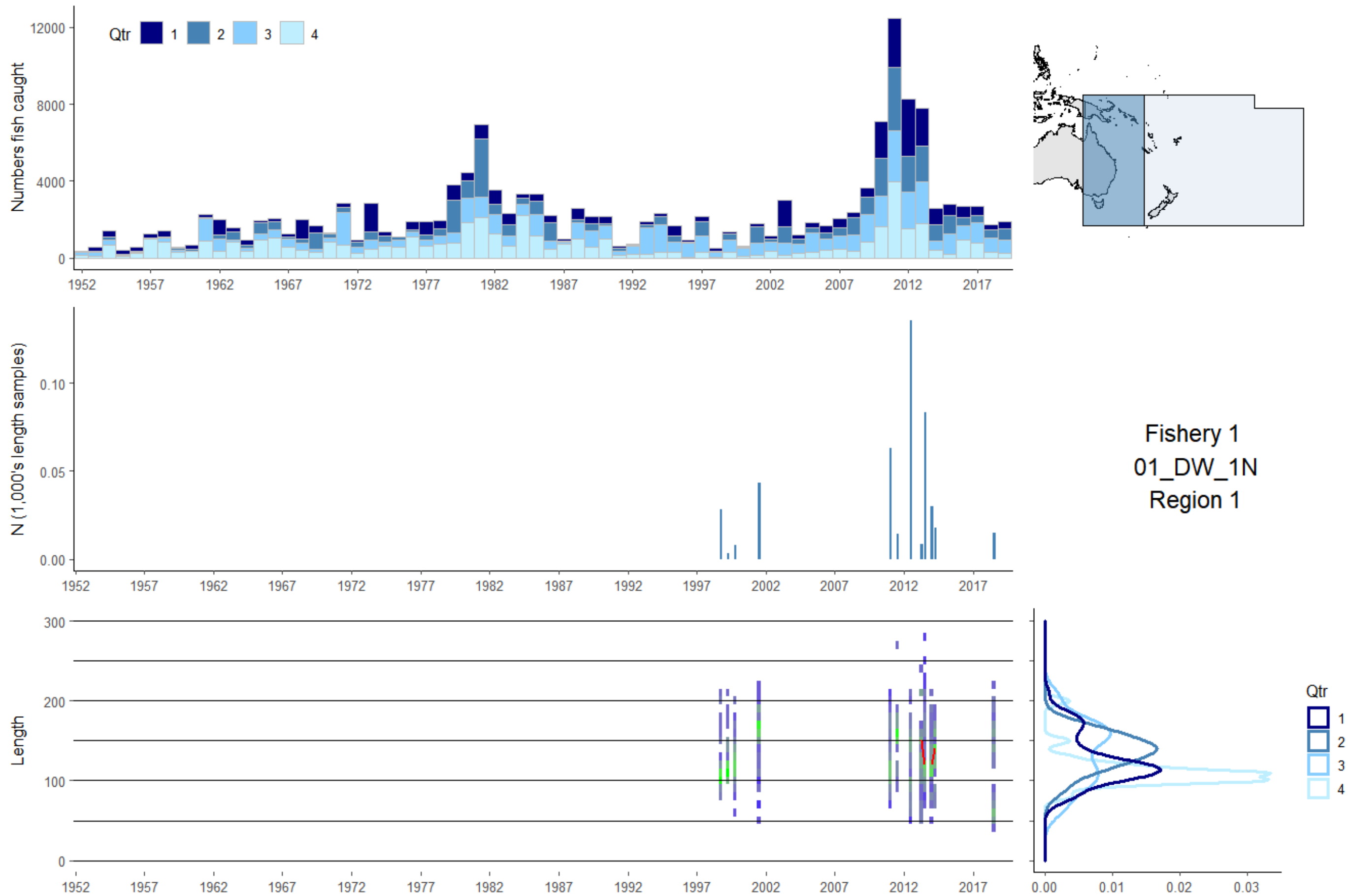

Figure A1-1: Summary plot of catch of swordfish (in numbers or weight), the number of size samples available, and the size distribution of fish measured or weighed, for fishery 1.

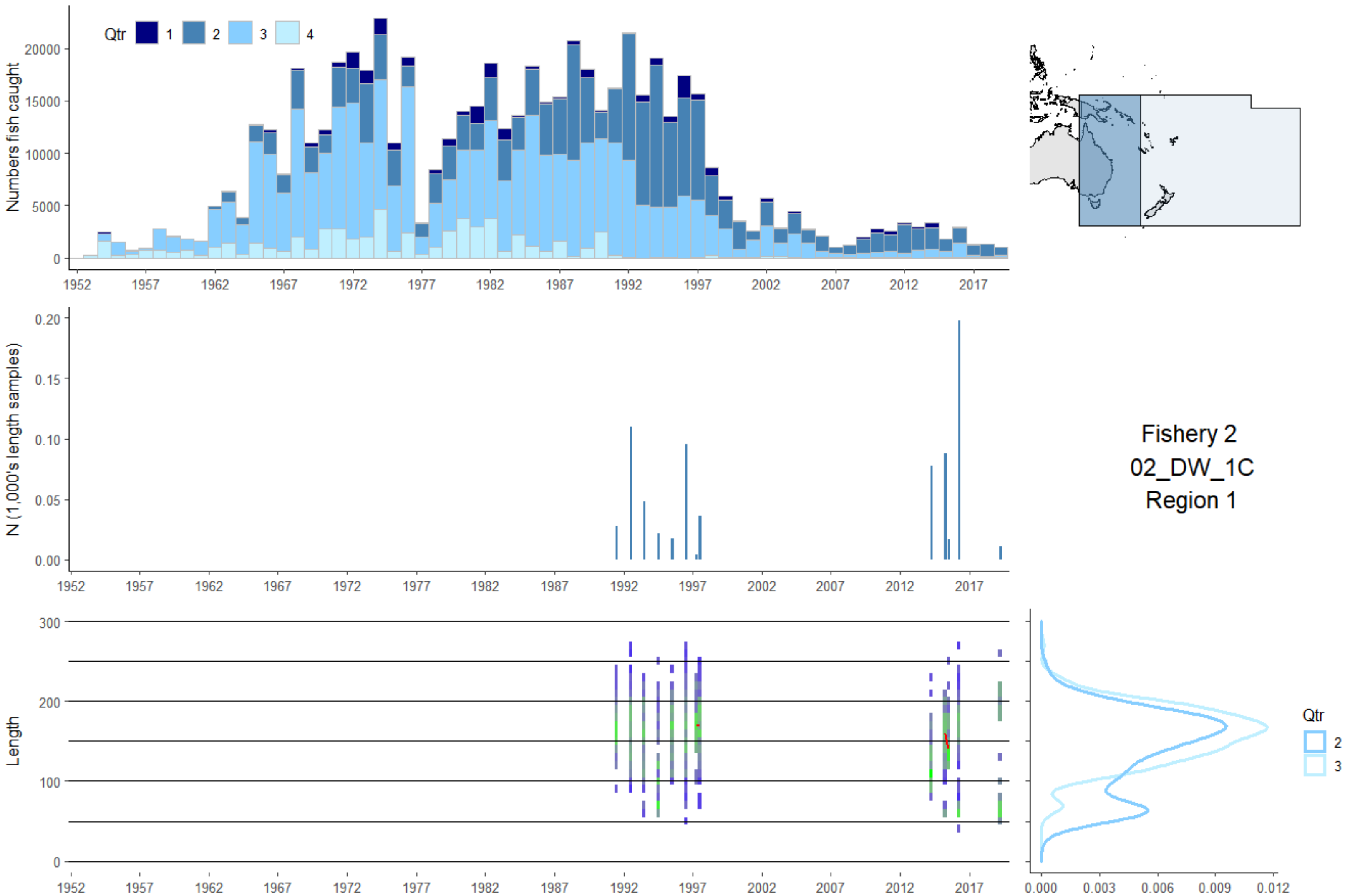

Figure A1-2: Summary plot for fishery 2.

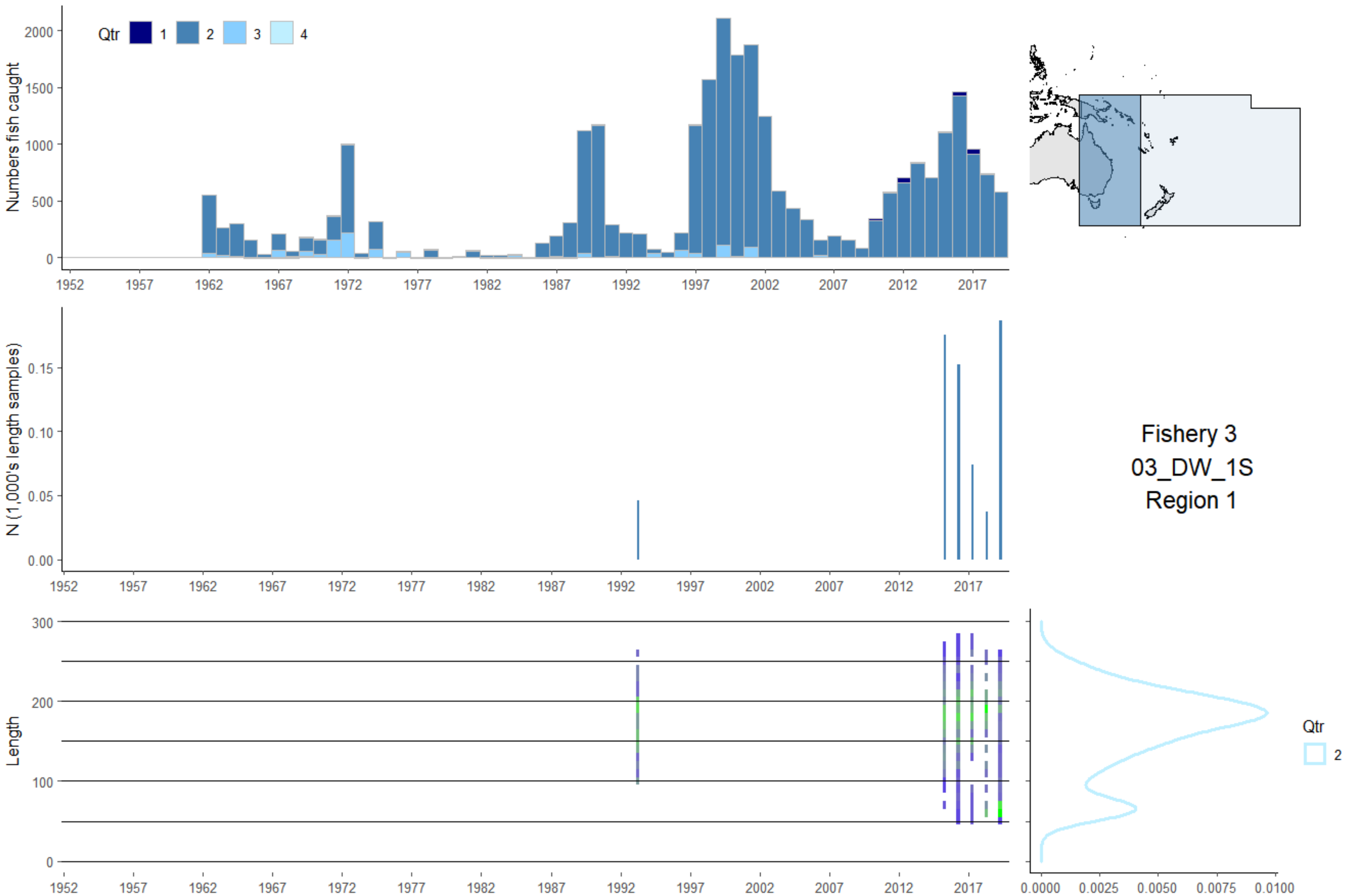

Figure A1-3: Summary plot for fishery 3.

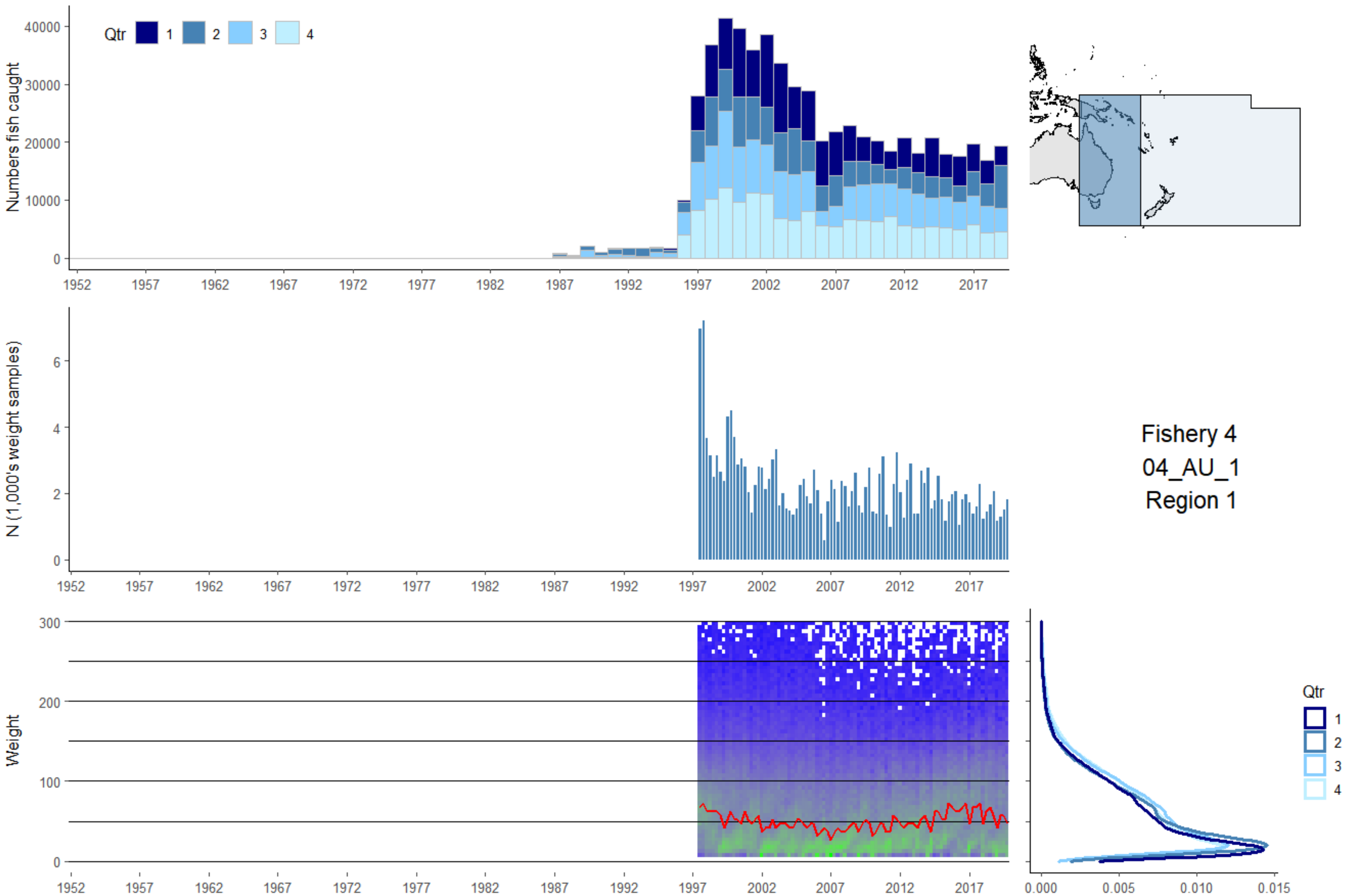

Figure A1-4: Summary plot for fishery 4.

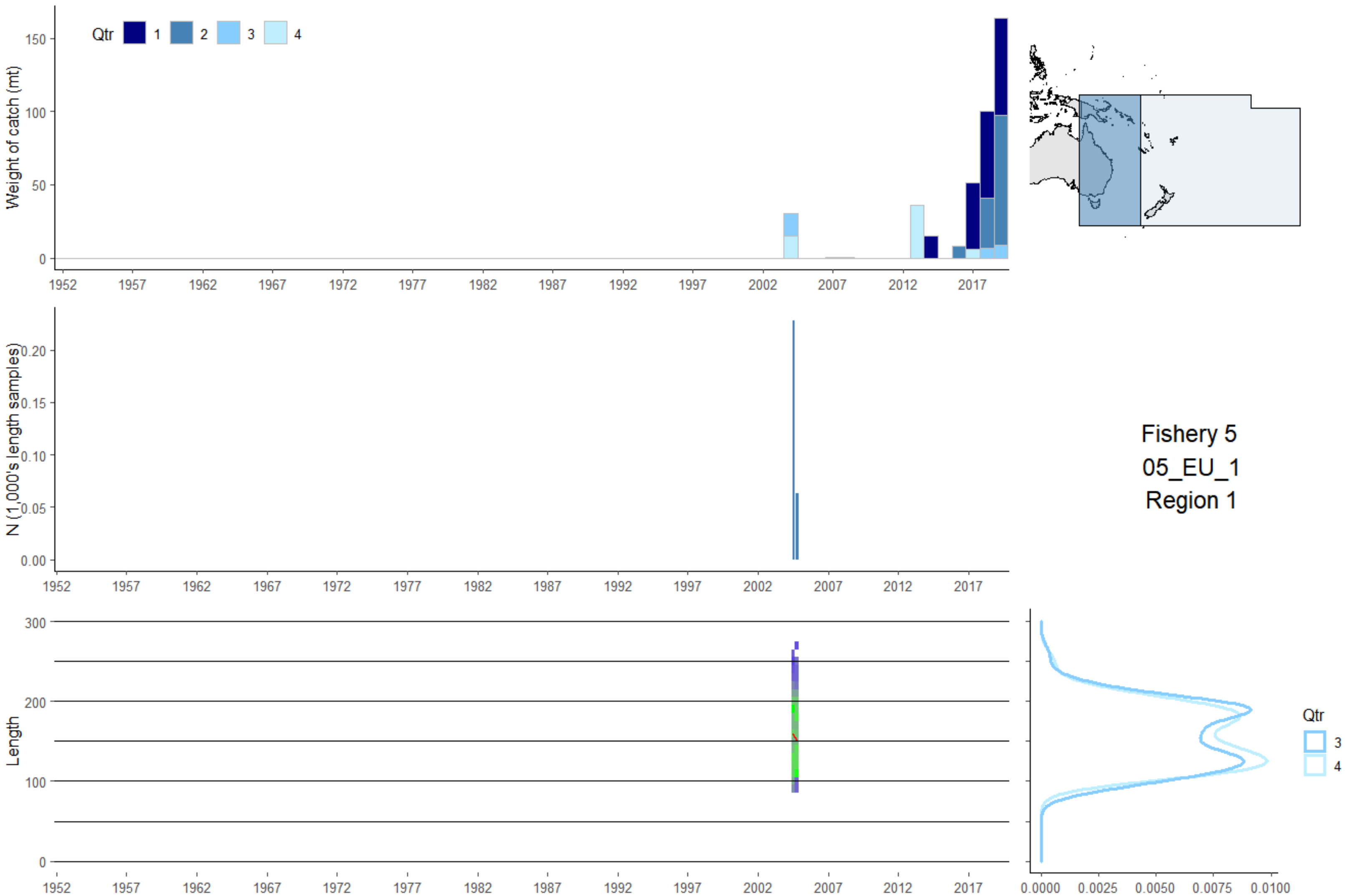

Figure A1-5: Summary plot for fishery 5.

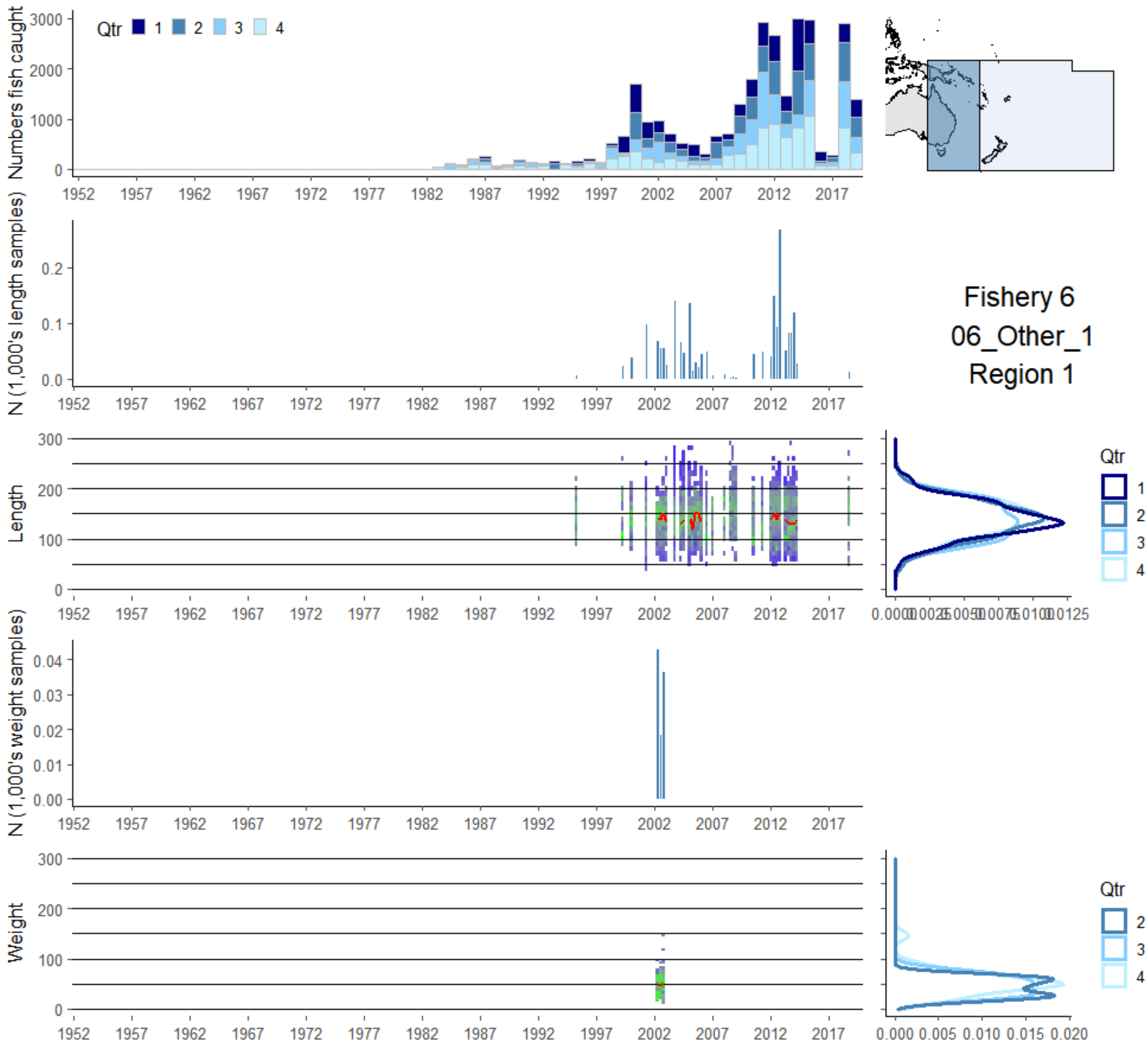

Figure A1-6: Summary plot for fishery 6.

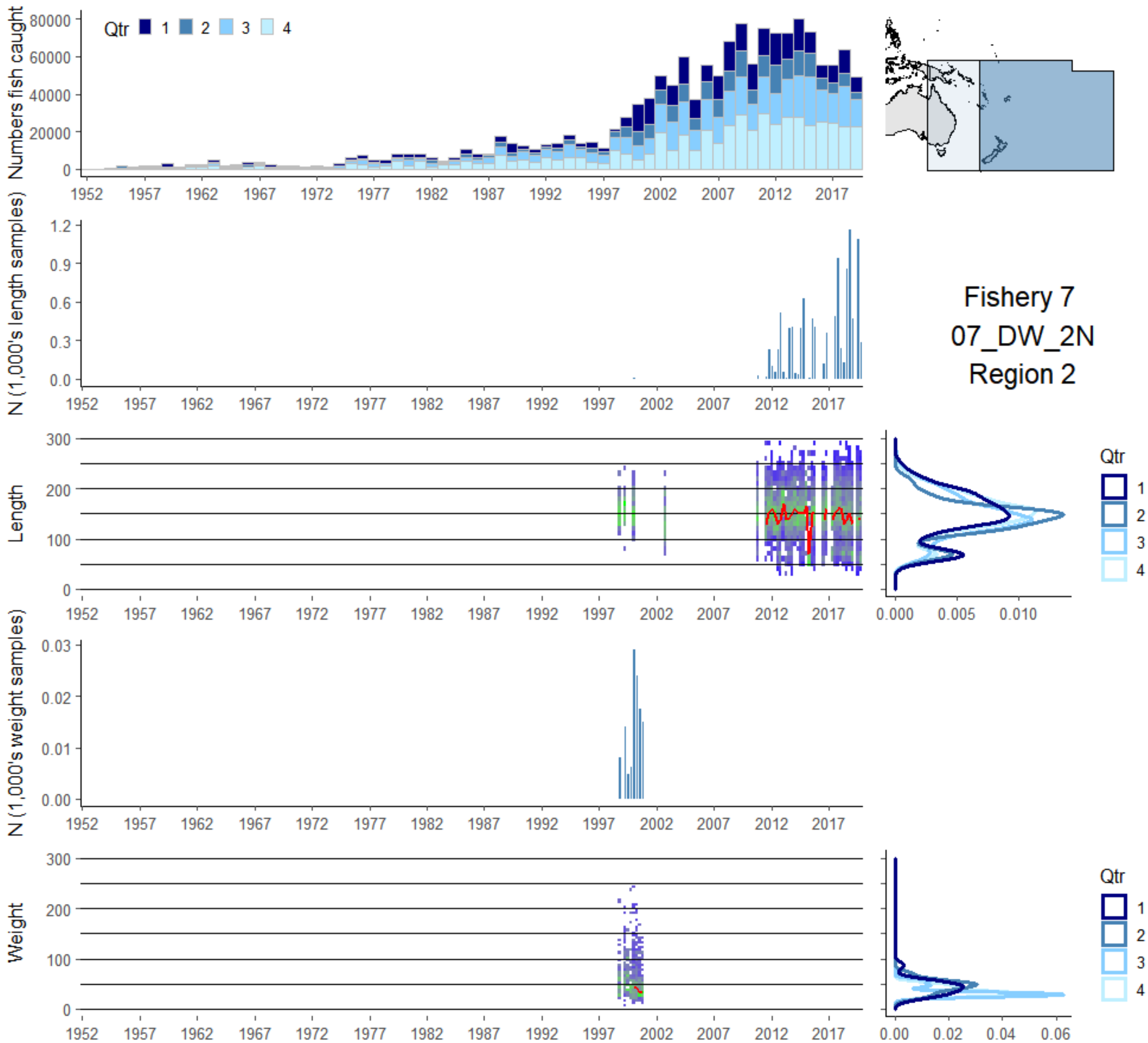

Figure A1-7: Summary plot for fishery 7.

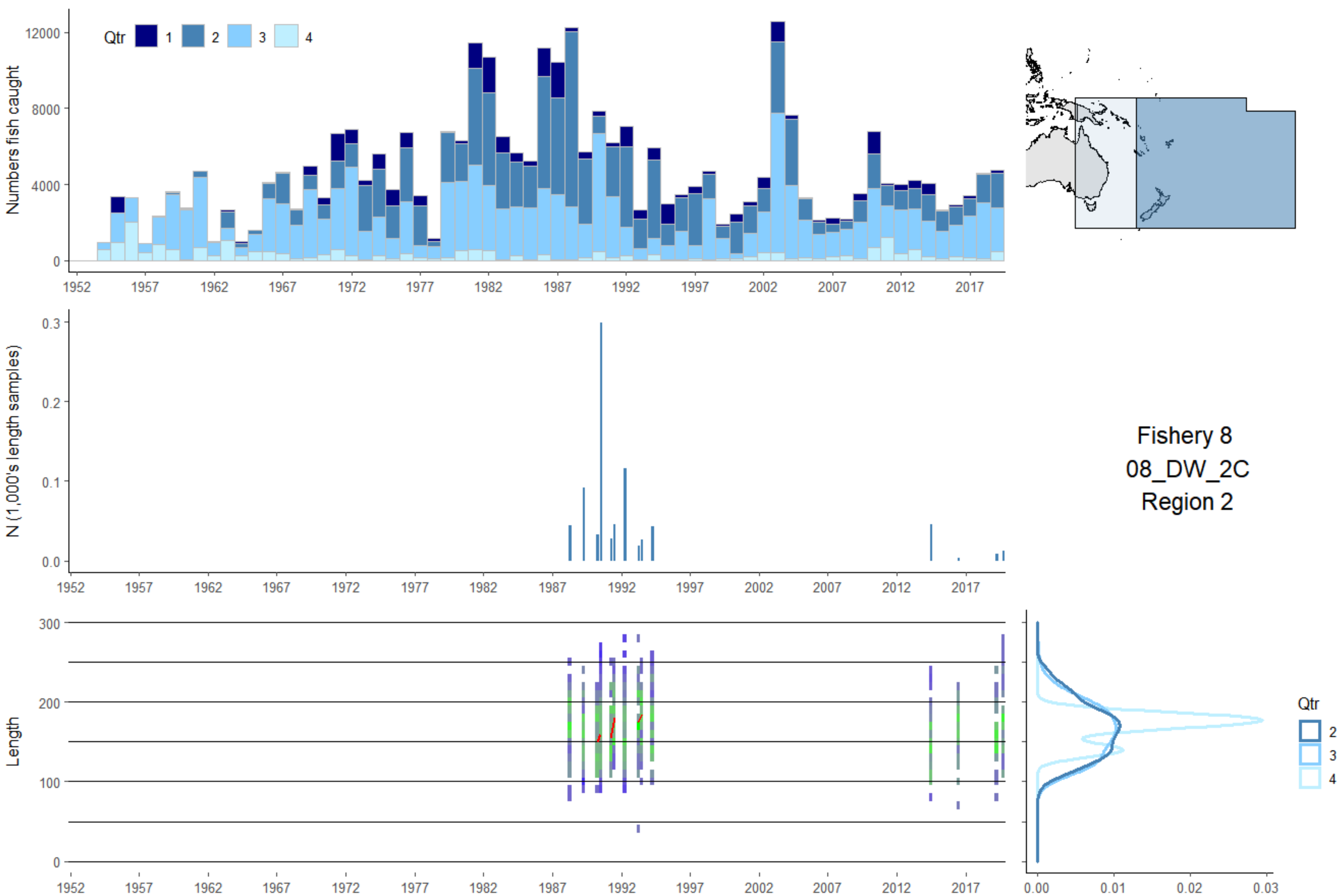

Figure A1-8: Summary plot for fishery 8.

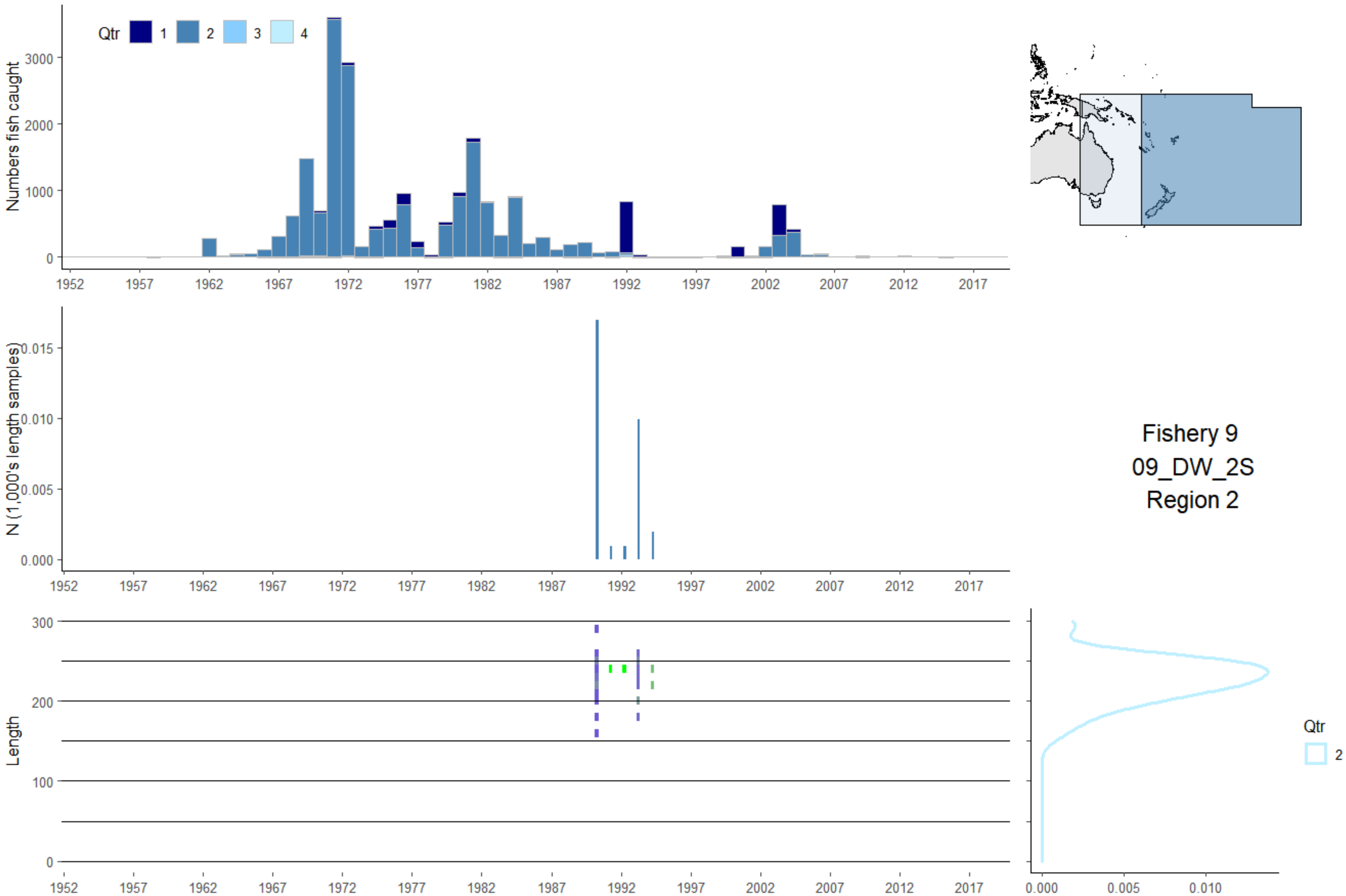

Figure A1-9: Summary plot for fishery 9.

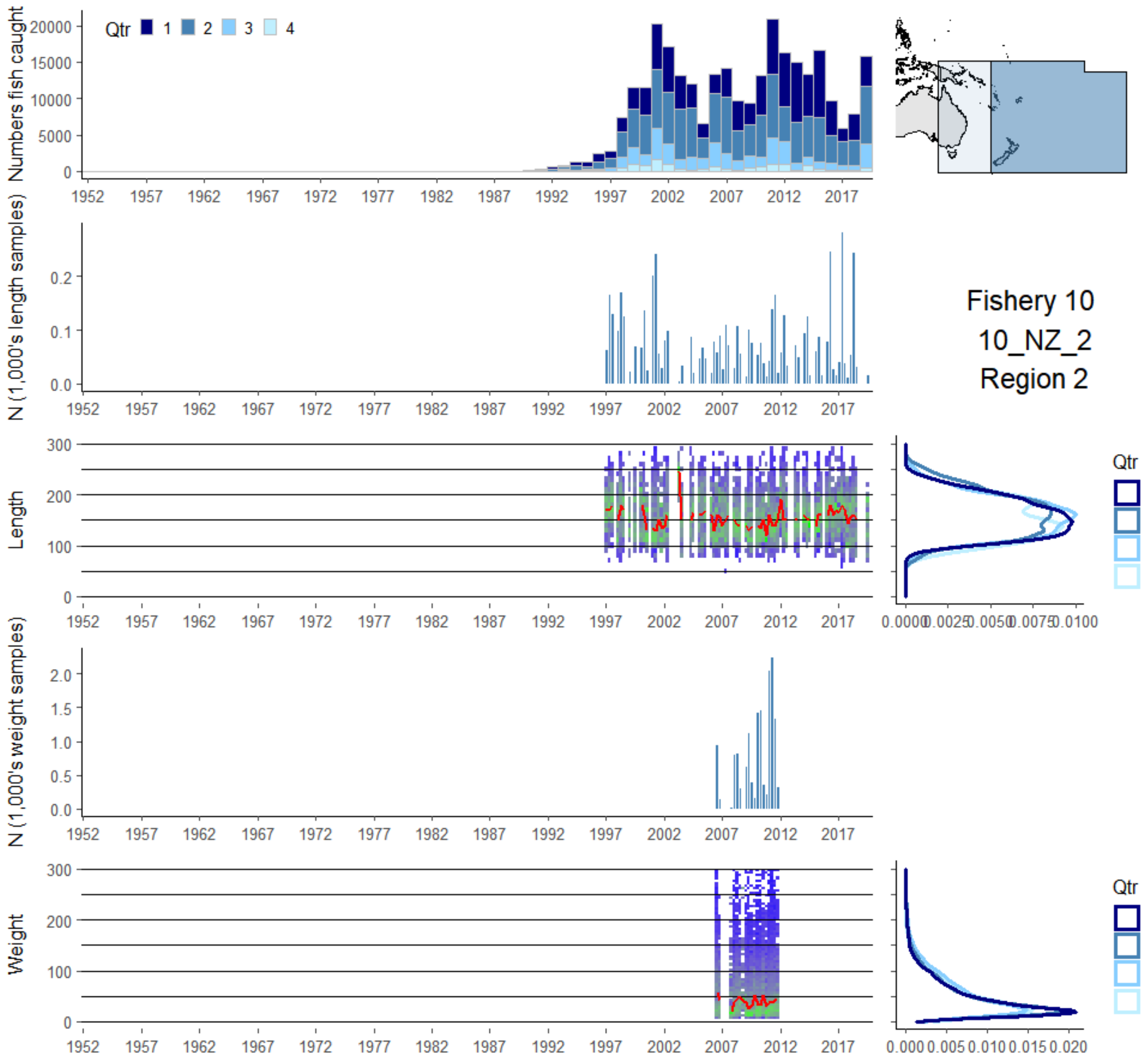

Figure A1-10: Summary plot for fishery 10.

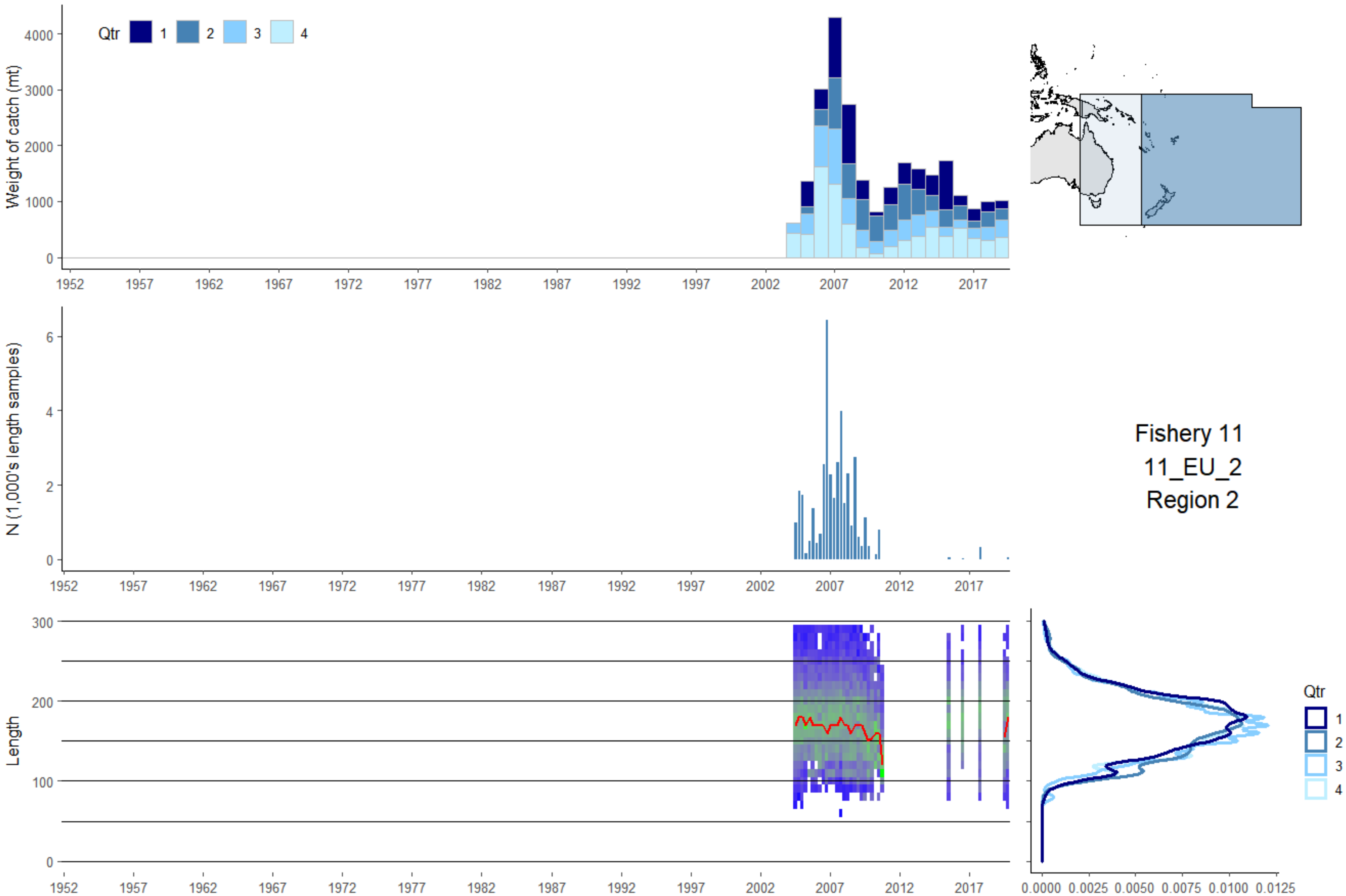

Figure A1-11: Summary plot for fishery 11.

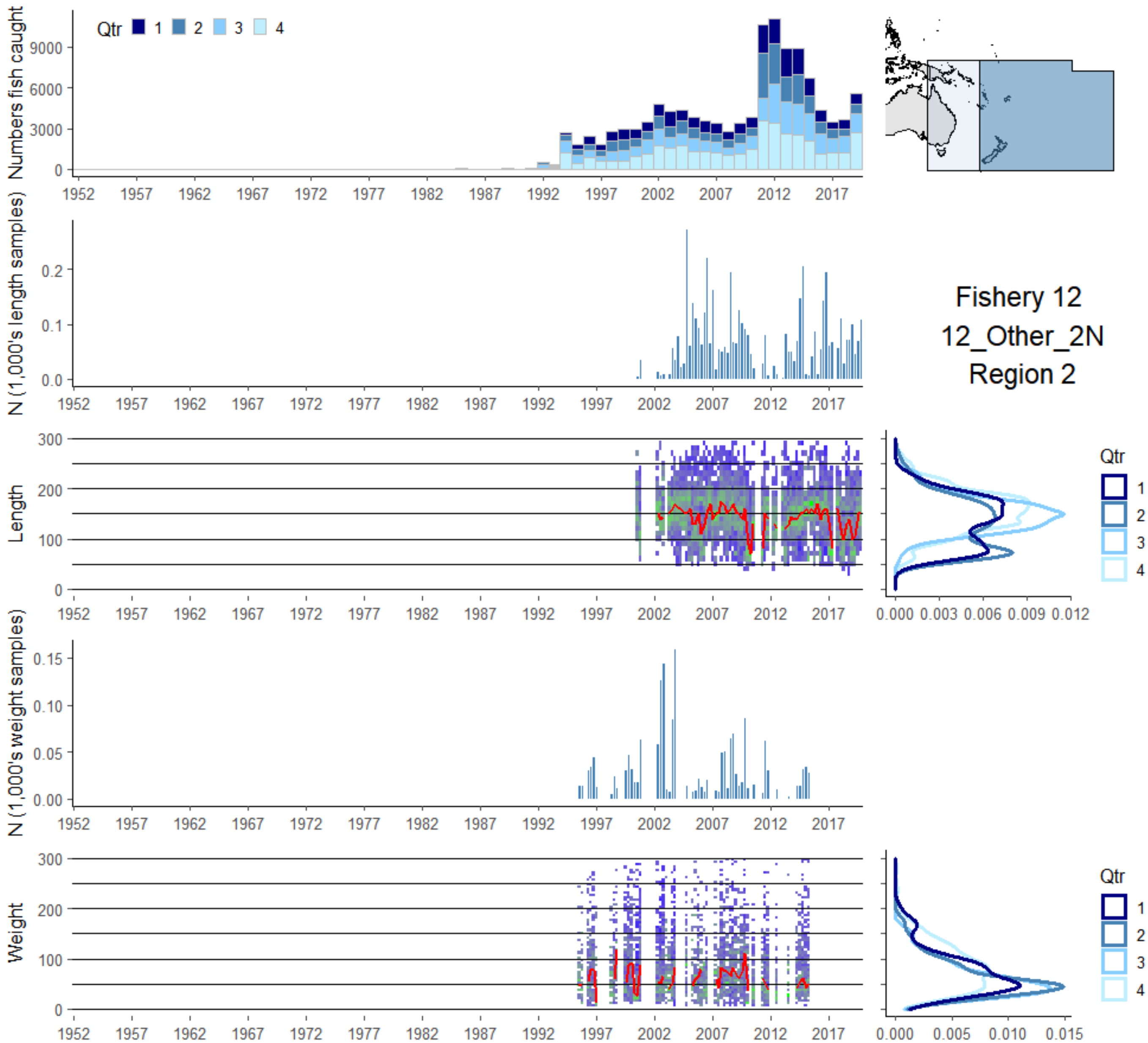

Figure A1-12: Summary plot for fishery 12.

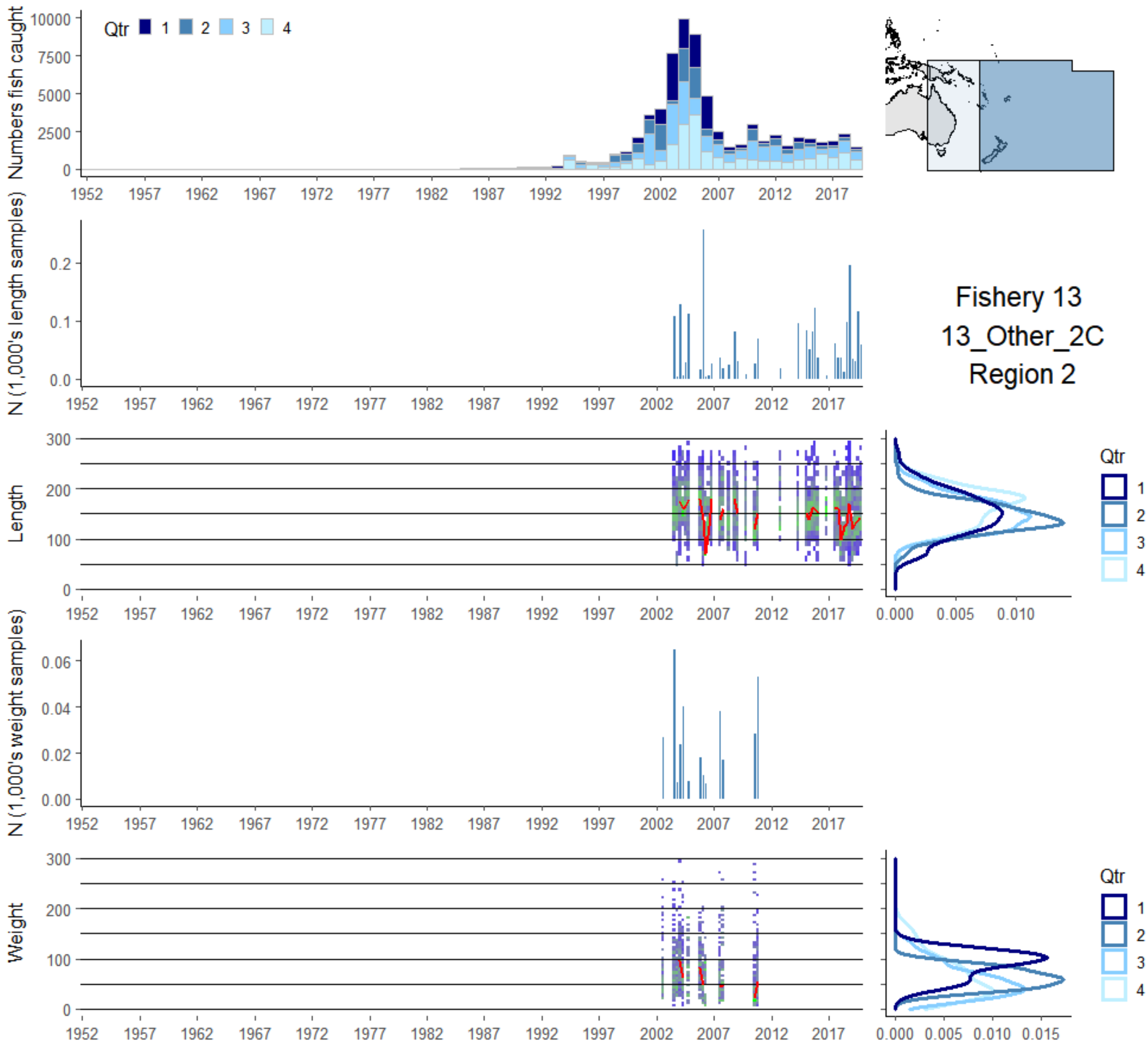

Figure A1-13: Summary plot for fishery 13.

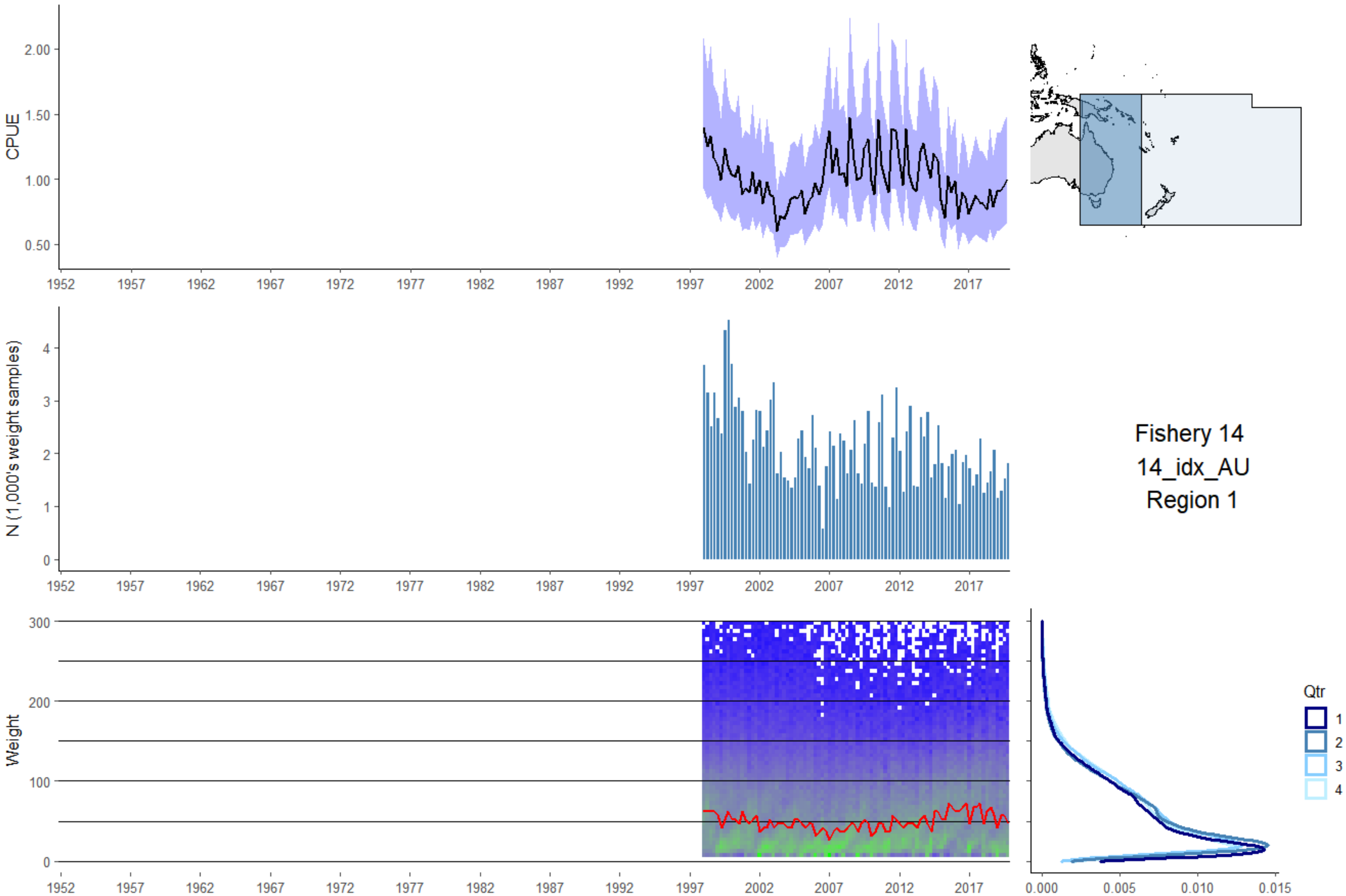

Figure A1-14: Summary plot for fishery 14.

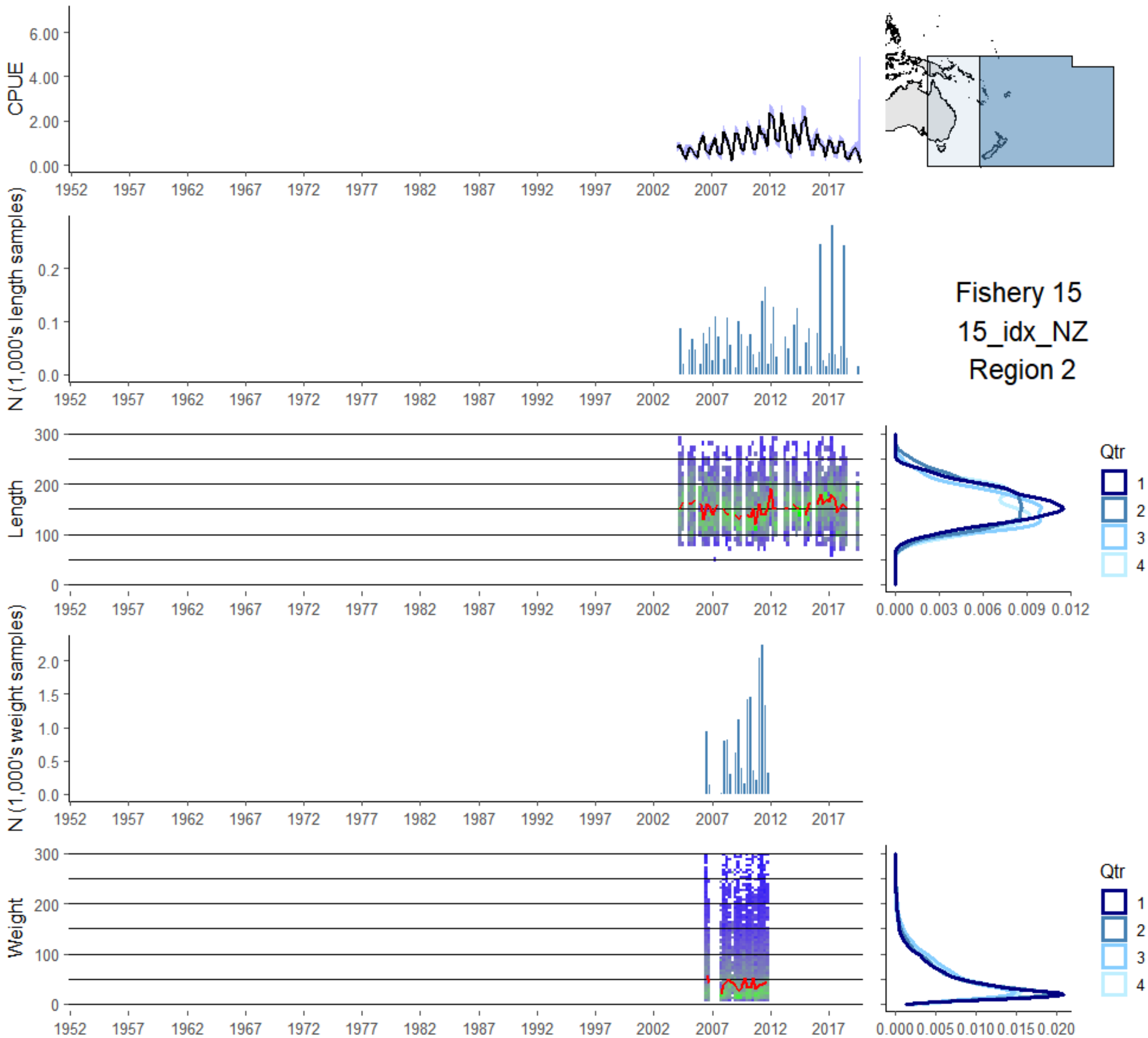

Figure A1-15: Summary plot for fishery 15.

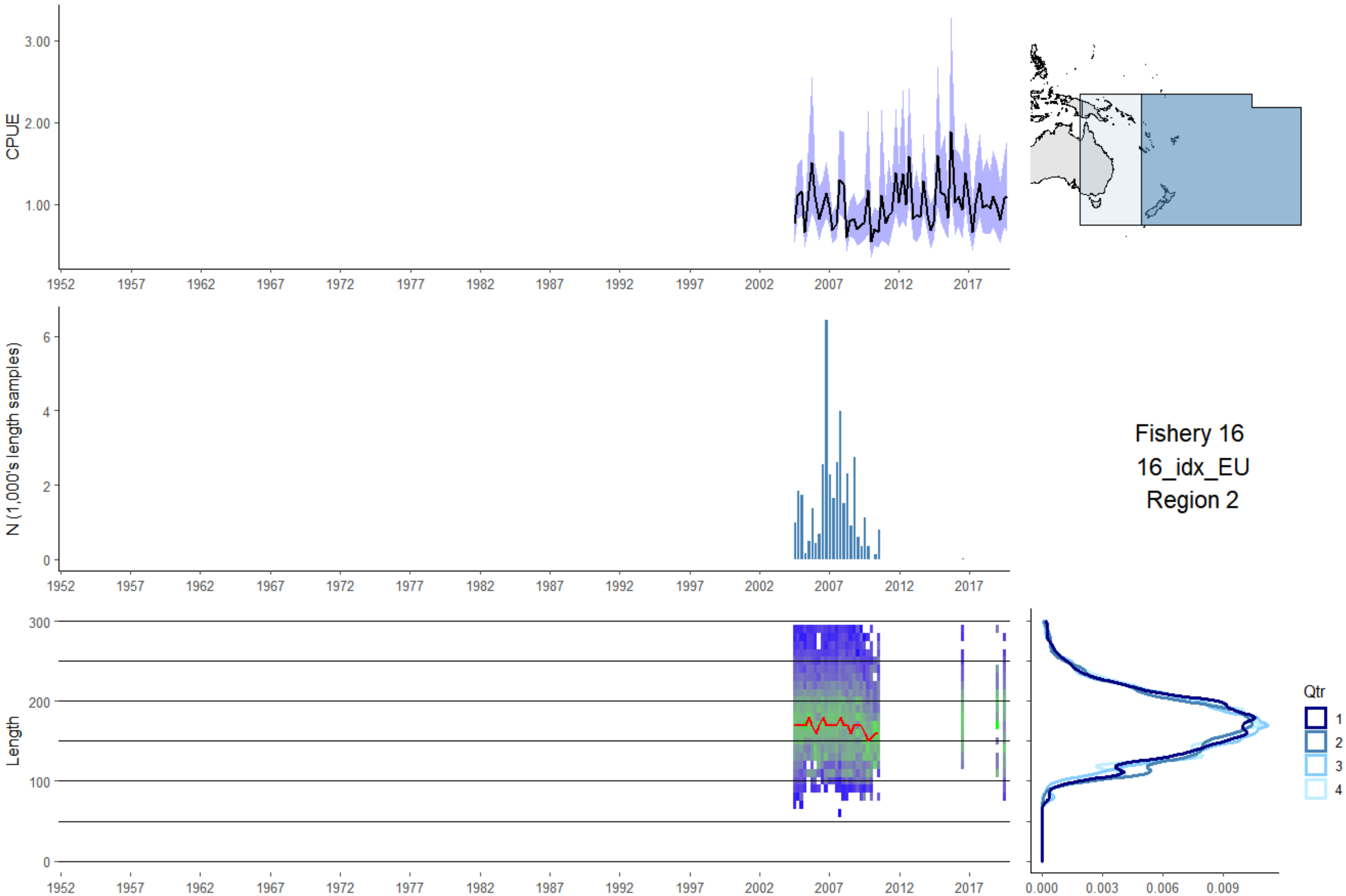

Figure A1-16: Summary plot for fishery 16.

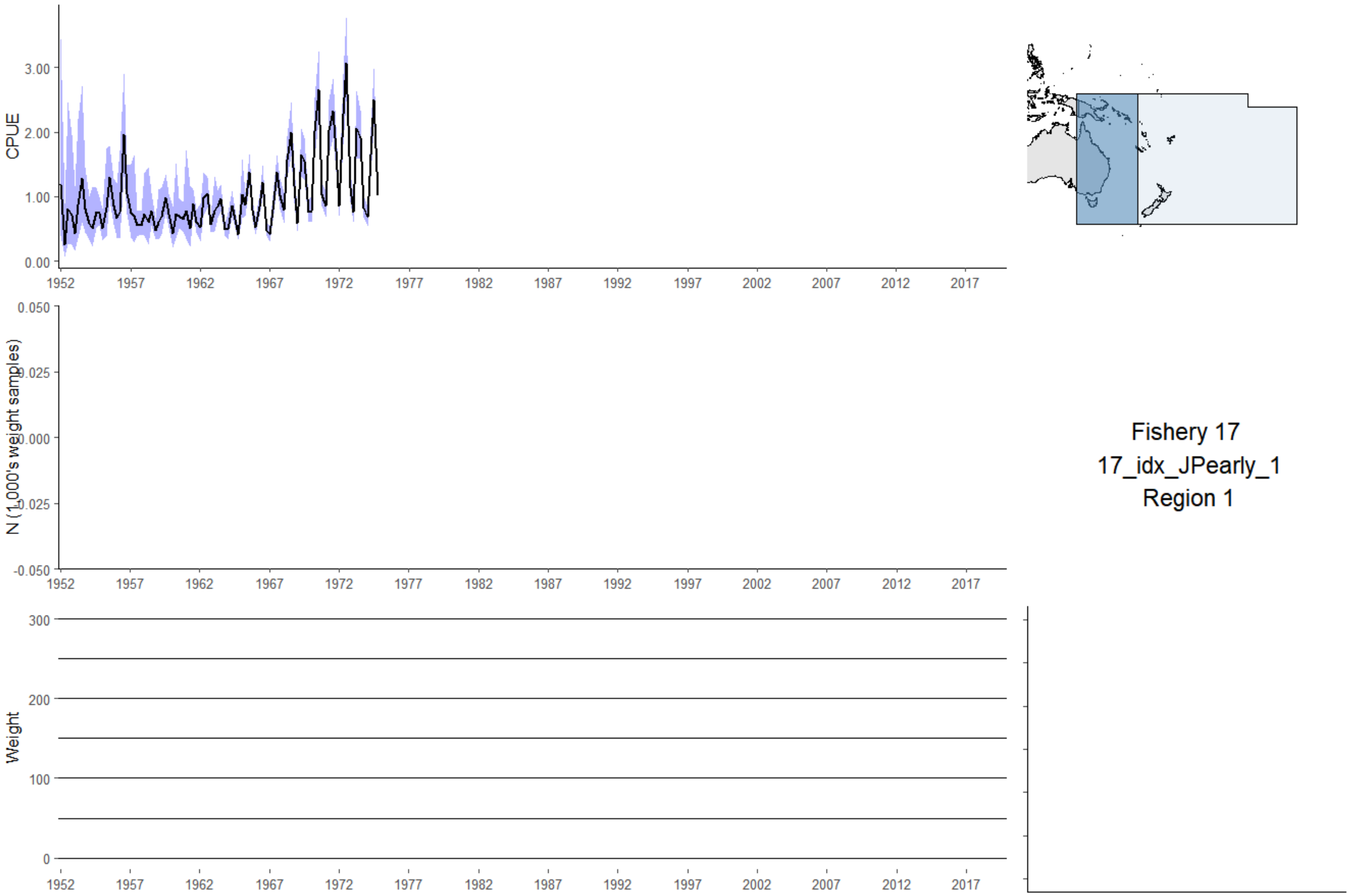

Figure A1-17: Summary plot for fishery 17.

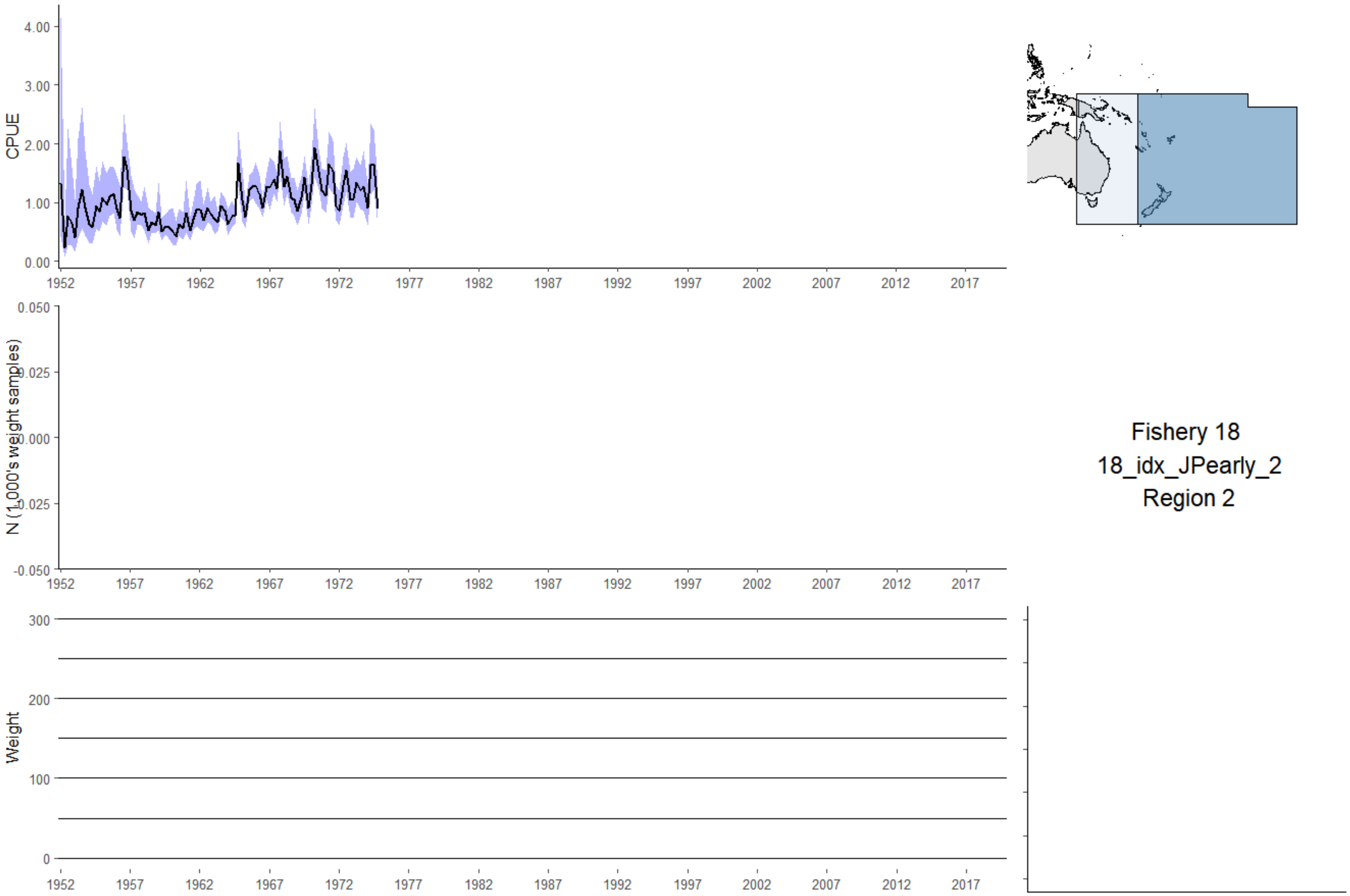

Figure A1-18: Summary plot for fishery 18.

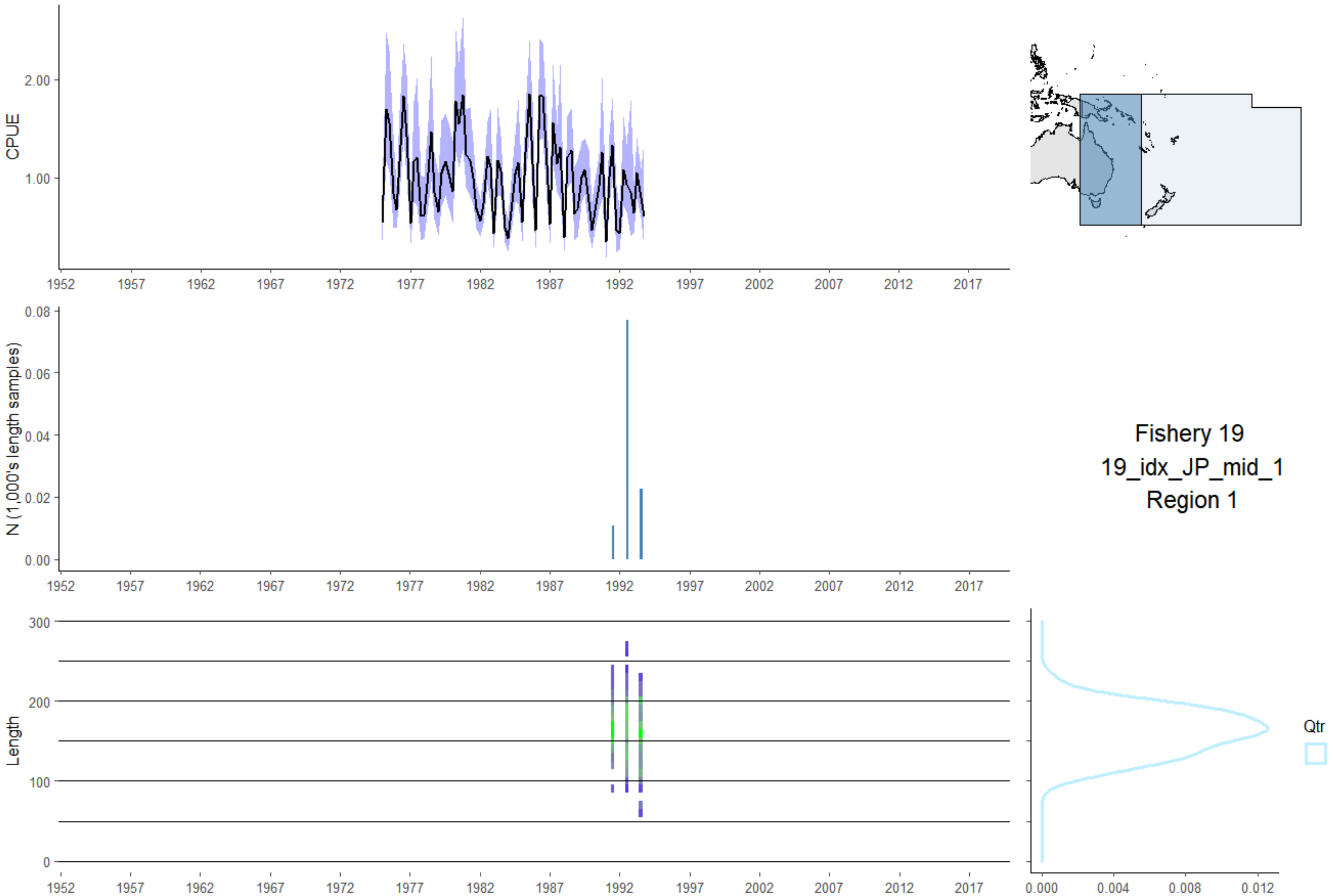

Figure A1-19: Summary plot for fishery 19.

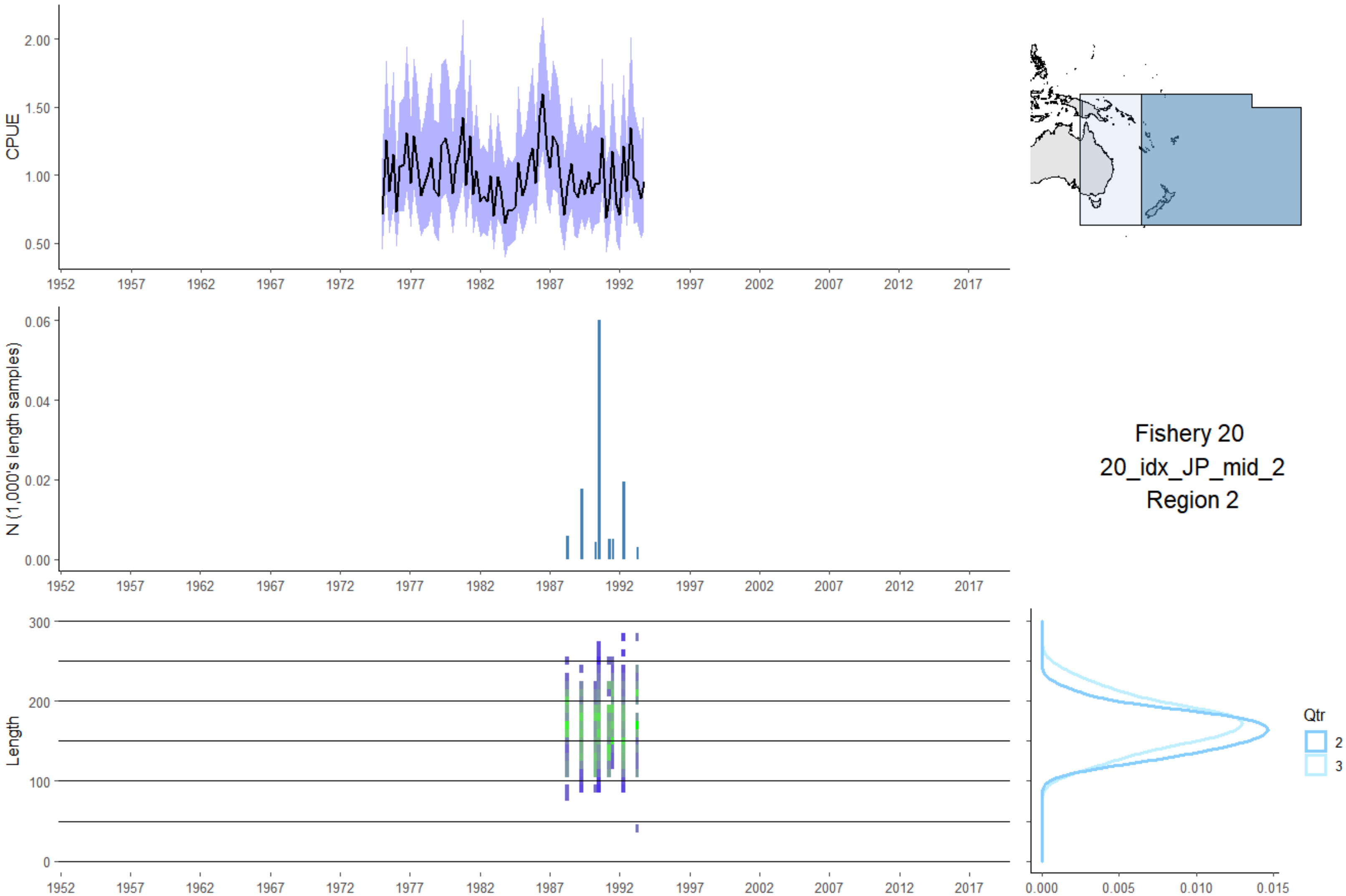

Figure A1-20: Summary plot for fishery 20.

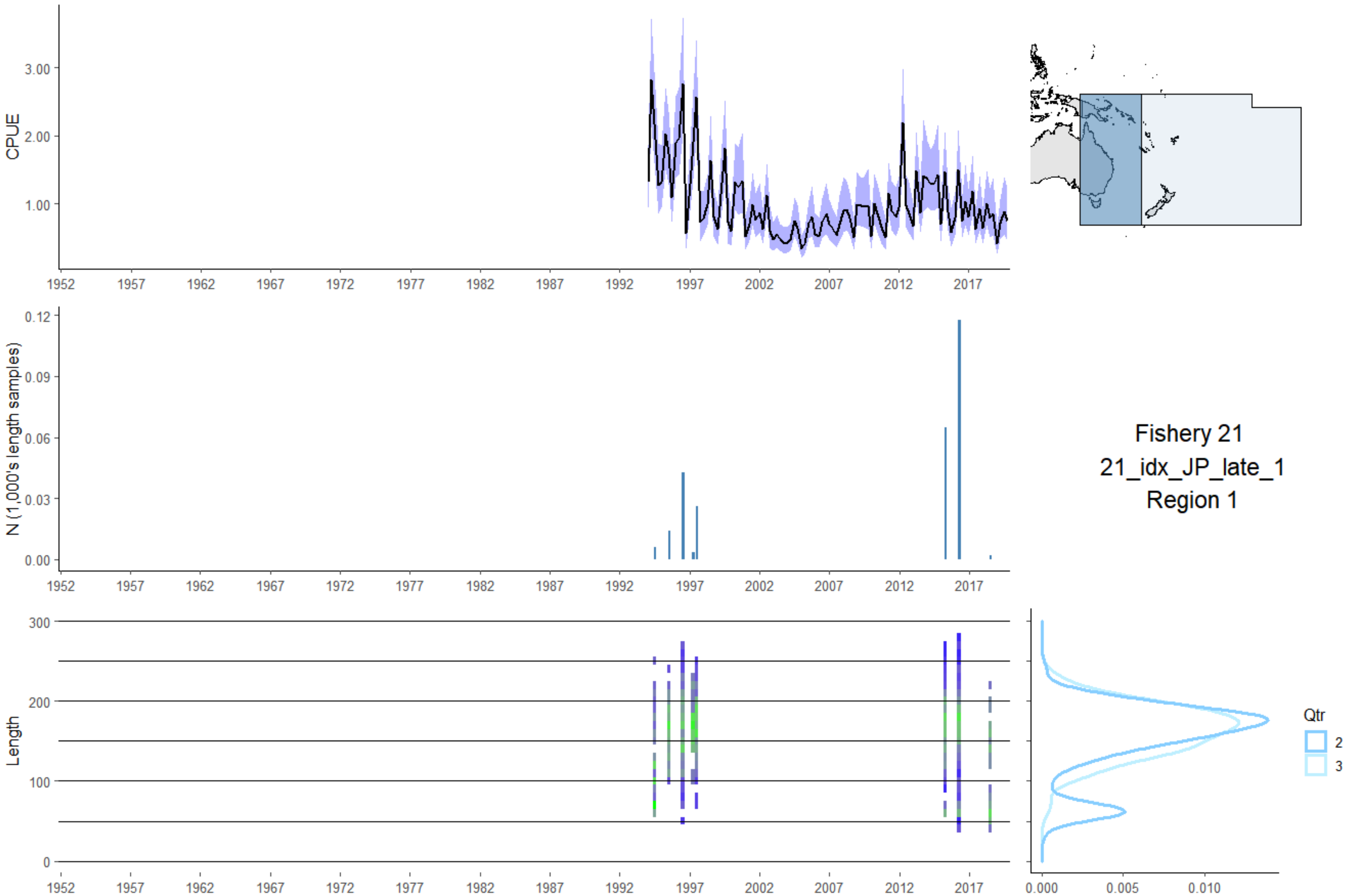

Figure A1-21: Summary plot for fishery 21.

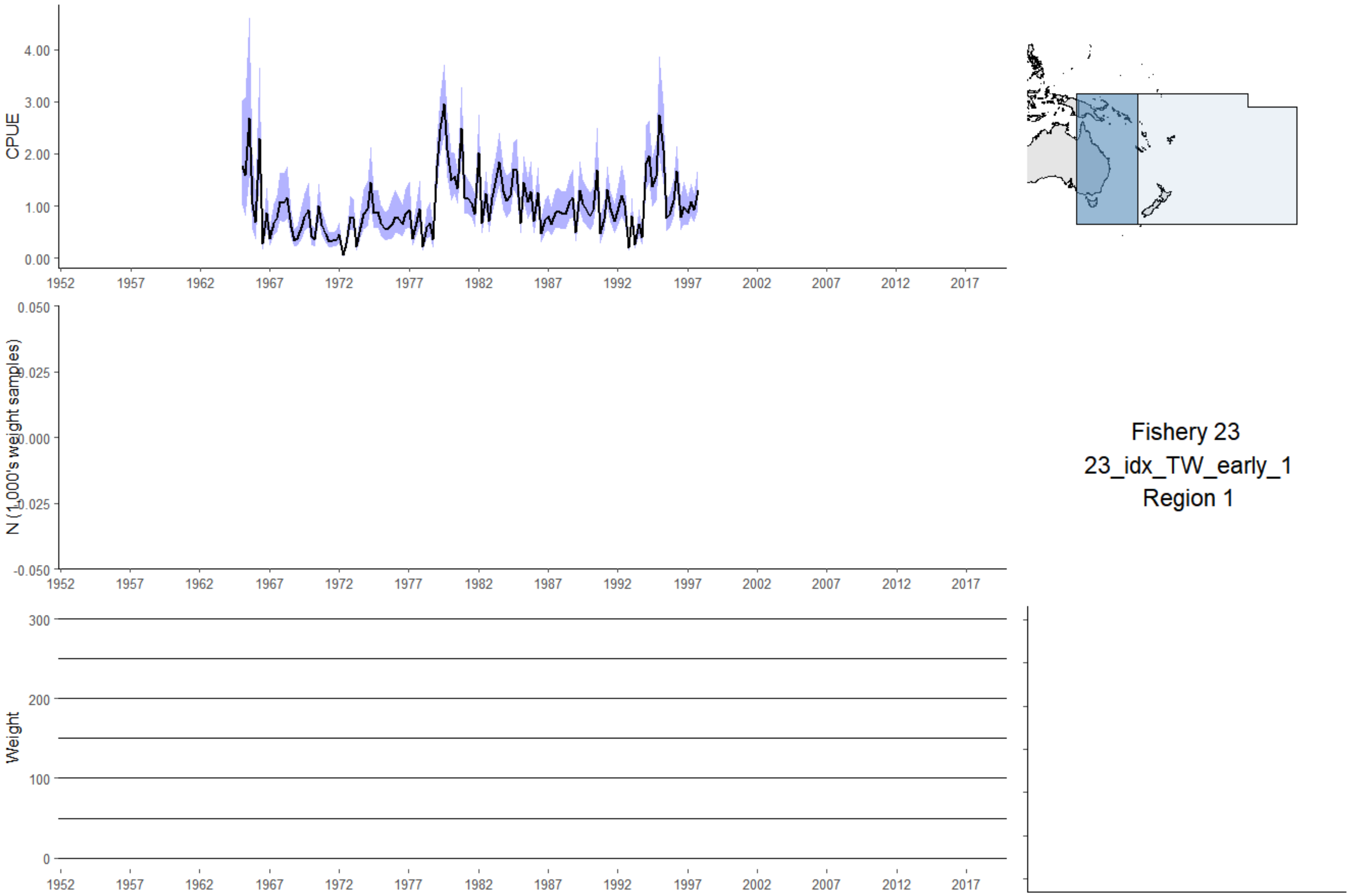

Figure A1-22: Summary plot for fishery 23.

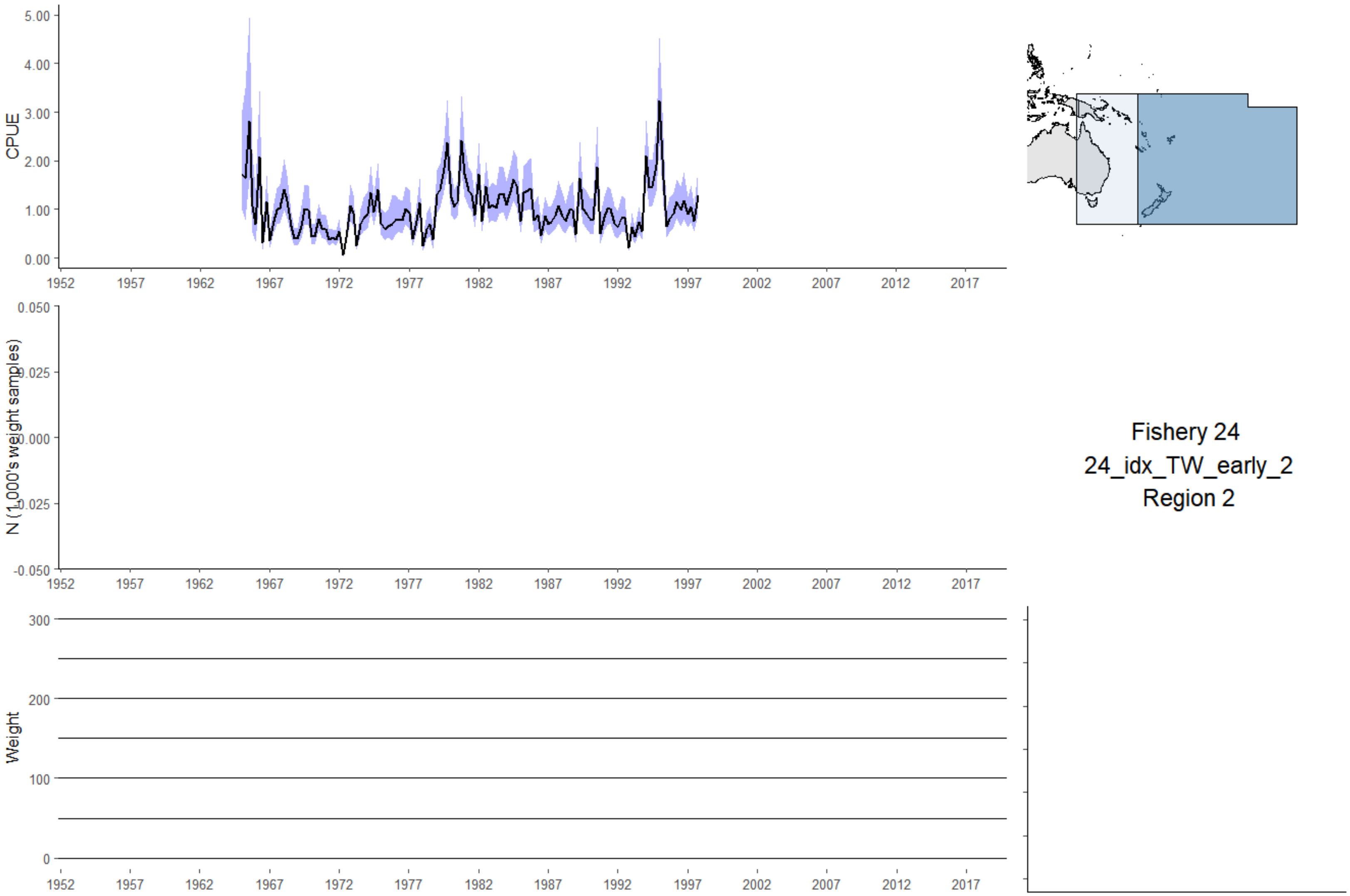

Figure A1-23: Summary plot for fishery 24.

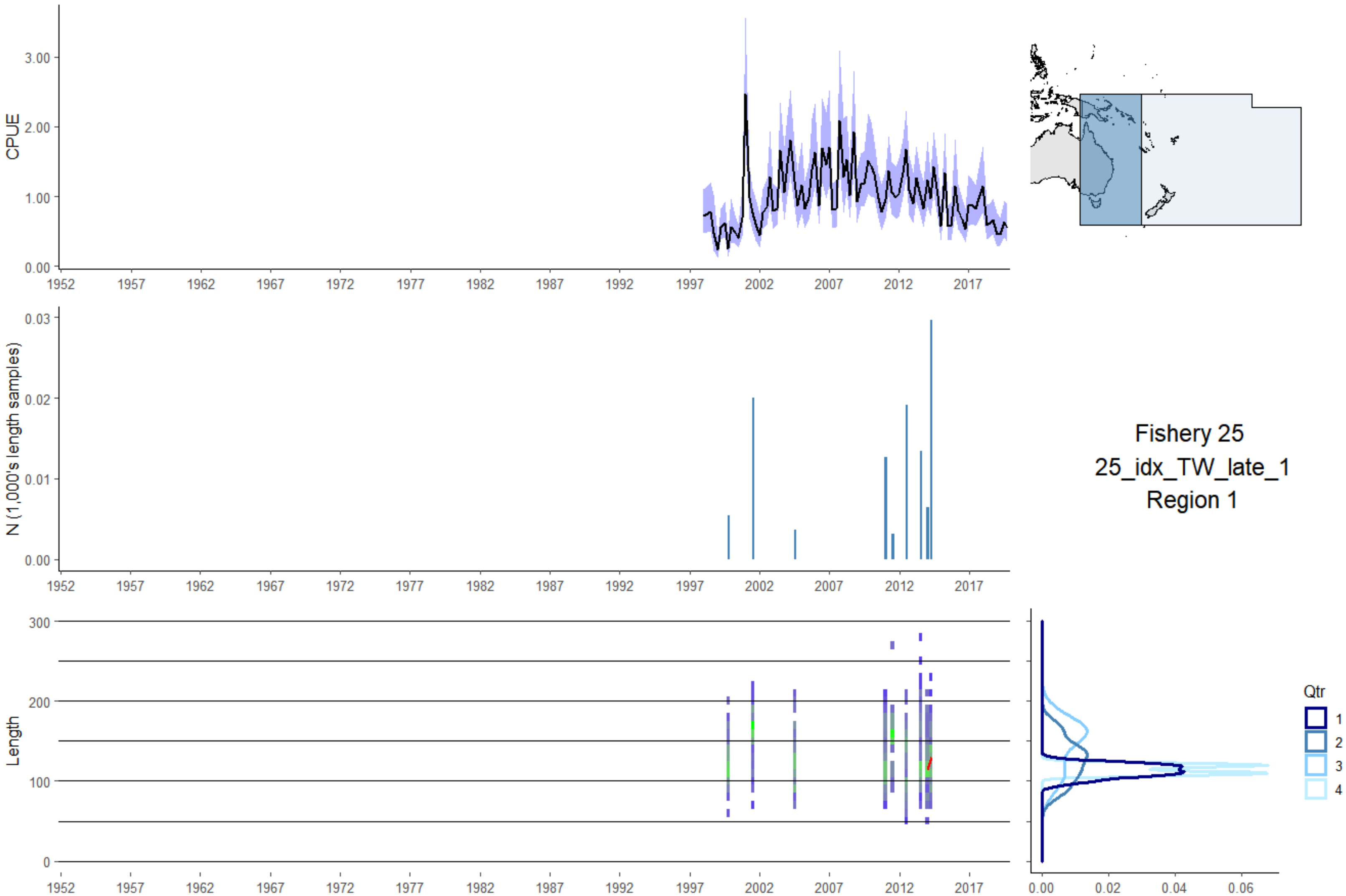

Figure A1-24: Summary plot for fishery 25.

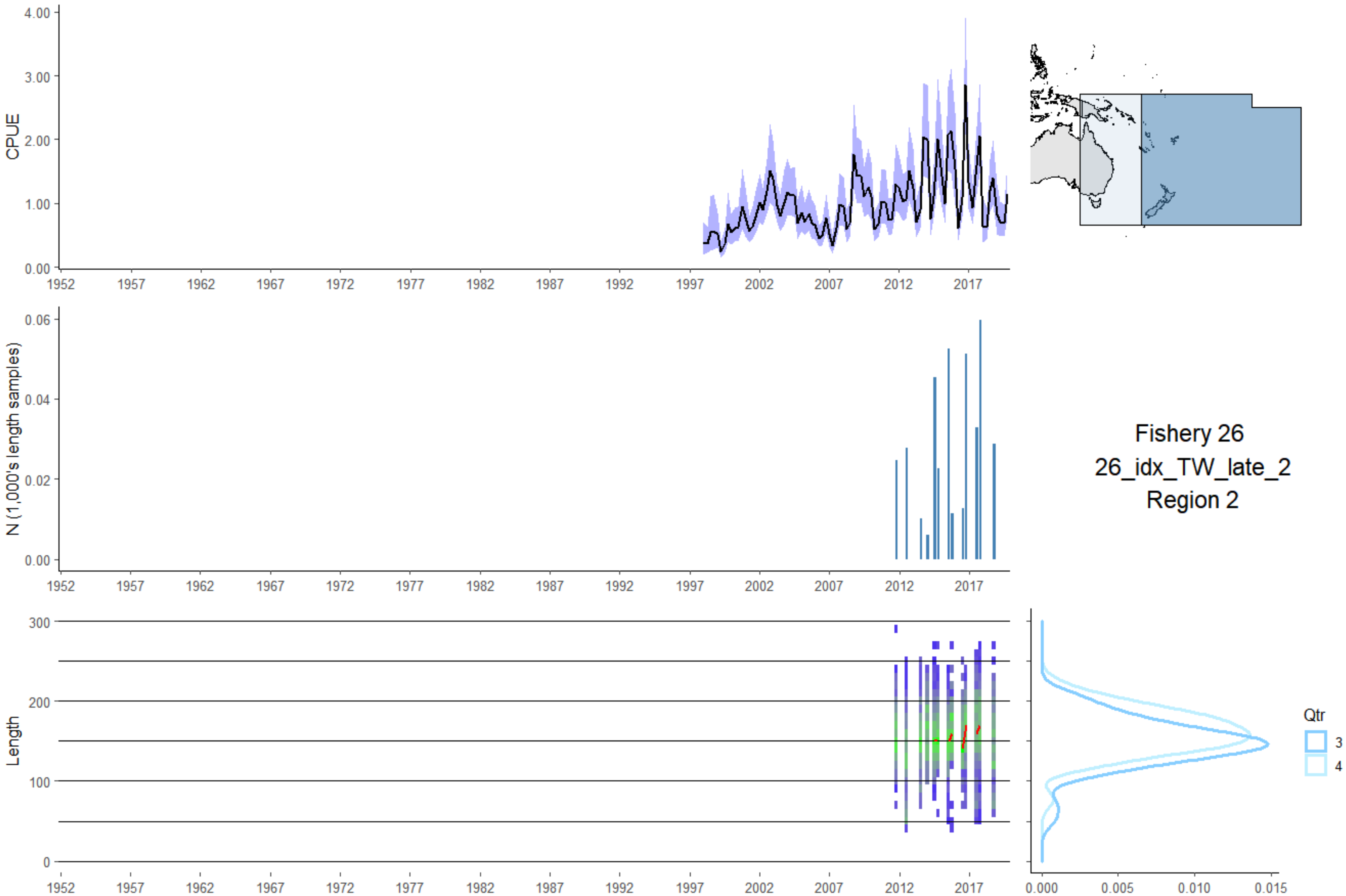

Figure A1-25: Summary plot for fishery 26.